CHALMERS
UNIVERSITY OF TECHNOLOGY

# On the antioxidant activity of lignin and the structural impacts

Master's thesis in Biotechnology

Paria Asadzadehkhaneghah

DEPARTMENT OF CHEMISTRY AND CHEMICAL ENGINEERING

CHALMERS UNIVERSITY OF TECHNOLOGY
Gothenburg, Sweden 2025
www.chalmers.se

MASTER'S THESIS 2025

# On the antioxidant activity of lignin and the structural impacts

Paria Asadzadehkhaneghah


Forest Products and Chemical Engineering Unit
*Department of Chemistry and Chemical Engineering*
Chalmers University of Technology
Gothenburg, SE-41296
Sweden 2025

On the antioxidant activity of lignin and the structural impacts
Paria Asadzadehkhaneghah



Supervisor: Liyang Liu, Chalmers
Ahilan Manisekaran, Chalmers
Examiner: Liyang Liu, Chalmers

Master's Thesis 2025
Forest Products and Chemical Engineering Unit
Department of Chemistry and Chemical Engineering
Chalmers University of Technology
SE-412 96 Gothenburg
Telephone +46 31 772 1000

Cover: Lignin is an abundant natural resource existing in plants, including wood and grass. It is produced in large amounts (> 50 million tons) as a byproduct of the pulp and paper industry annually.[1] With its unique structure, lignin offers powerful antioxidant properties, making it a plentiful and sustainable antioxidant that nature has gifted us.[2] Photo taken by Felix Blomfelt.

Typeset in Microsoft word
Printed by Chalmers Reproservice
Gothenburg, Sweden 2025

On the antioxidant activity of lignin and the structural impacts
Paria Asadzadehkhaneghah
Department of Chemistry and Chemical Engineering
Chalmers University of Technology

# Abstract

The development of nature-based antioxidants is a crucial step toward a sustainable society, including lignin, an organic complex biopolymer in plants, offering versatile properties, particularly antioxidant characteristics. To effectively use lignin as a commercial antioxidant, it is essential to identify the specific structural features responsible for its antioxidant activity. The polyphenolic structure of lignin is particularly relevant, since these functional groups are found in many antioxidants. (e.g., vitamin E). This study investigates the correlation between phenolic hydroxyl group content (phenolic -OH) and antioxidant activity in seven types of lignin, including original and modified lignins. To quantify the phenolic-OH groups, conductometric titration and quantitative Phosphorus-31 nuclear magnetic resonance spectroscopy ($^{31}$P NMR) were performed. Antioxidant activity was assessed using DPPH(2,2-diphenyl-1-picrylhydrazyl) and ABTS (2,2′-azino-bis(3-ethylbenzothiazoline-6-sulfonic acid)) radical scavenging methodologies. Furthermore, linear regression, Pearson, Spearman, and Kendall's Tau correlation analyses were performed to evaluate the correlation between the number of phenolic -OH groups and antioxidant activity. Lastly, the results from Fourier transform infrared spectroscopy (FT-IR) were interpreted to investigate the presence of other lignin structures/functional groups that might influence antioxidant activity.

A strong linear correlation between titration and $^{31}$P NMR results ($R^2$ = 0.97) reveals that conductometric titration can be a suitable quantitative method for measuring phenolic-OH content. Correlation results ($R^2$ = 0.51 for phenolic content vs DPPH; $R^2$= 0.66 for phenolic content vs ABTS) indicate that the phenolic-OH content has a moderate effect on antioxidant activity, but it is not always the dominant factor. Other correlation analyses, including Kendall's Tau, Pearson, and Spearman, have been performed in the study and have shown similar trends. For instance, hydroxyethyl softwood kraft lignin (the modified lignin without any phenol groups) shows comparable antioxidant properties to the original lignin. This finding ultimately suggests that other structural factors, such as chromophores (conjugation and carbonyl groups), may play a crucial role in lignin antioxidant activity.

Keywords: Lignin, phenolic content characterization, antioxidant activity, titration, $^{31}$P NMR, FT-IR, DPPH, ABTS, chromophore, conjugated carbonyl.

# Acknowledgements

I would like to express my deepest gratitude to my supervisors, **Liyang Liu** and **Ahilan Manisekaran**, for their invaluable guidance, unwavering support, and constant encouragement throughout this research. Their wisdom and expertise have been a source of inspiration, and I am truly fortunate to have had their mentorship.

I am also profoundly grateful to **Yuge Yao** and **Elahe Sharifi** for their generous support, insightful guidance, and kindness during my thesis journey. Your patience and willingness to help have made this experience both enriching and rewarding.

I would also like to thank **Emilia Rózsa**, without whom I wouldn't be where I am today.

Most importantly, I would like to thank my family for their unconditional love and support. Their belief in me has been my greatest strength.

This journey has been one of growth, challenges, and discoveries, and I could not have navigated it without such incredible mentors and friends. Thank you for your belief in me, your time, and your unwavering support. I will always cherish the knowledge and experiences gained along the way.

Paria Asadzadehkhaneghah, Gothenburg, April 2025

# List of Acronyms

Below is the list of acronyms that have been used throughout this thesis listed in alphabetical order:

| | |
|---|---|
| ABTS | 2,2′-azino-bis (3-ethylbenzothiazoline-6-sulfonic acid) |
| A | Absorbance |
| DPPH | 2,2-diphenyl-1-picrylhydrazyl |
| FT-IR | Fourier transform infrared spectroscopy |
| $^{31}$P NMR | Phosphorous nuclear magnetic resonance spectroscopy |
| RSA | Radical scavenging activity |
| BDE | Bond dissociation energy |
| wt. | Weight |
| $M_w$ | Weight average molecular weight |
| DS | Degree of substitution |
| $M_n$ | Number average molecular weight |
| OSHL | Organoslov hardwood lignin |
| SKL1 | Softwood kraft lignin 1 |
| SKL2 | Softwood kraft lignin 2 |
| SKL3 | Softwood kraft lignin 3 |
| HEOSHL | Hydroxyethyl organosolv hardwood lignin |
| HESKL1 | Hydroxyethyl softwood kraft lignin |
| Amine SKL3 | Aminated softwood kraft lignin |
| BHA | Butylated hydroxyanisole |
| BHT | Butylated hydroxytoluene |
| PG | Propyl gallate |
| TBHQ | Tert-butyl hydroquinone |
| EHL | Enzymatic hydrolysis Lignin |
| HAT | Hydrogen atom transfer |
| SET | Single electron transfer |
| SPLET | Sequential proton loss electron transfer |
| PCET | Proton coupled electron transfer |
| IS | Internal standard |
| $R^2$ | Coefficient of determination |
| SST | Total sum of squares |
| SSR | Regression sum of squares |
| SSE | Error sums of squares |
| $\hat{\rho}(r)$ | Sample Pearson correlation coefficient between u and v |

# Nomenclature

Below is the nomenclature of indices, sets, parameters, and variables that have been used throughout this thesis.

## Sets

| Symbol | Description | Unit |
|---|---|---|
| $\{y_i\}$ | Set of all experimental data points | - |
| $\{\hat{y}_i\}$ | Set of all model-predicted values | - |
| $\{u_i\}$ | Sets of observed $u$ data points | - |
| $\{v_i\}$ | Sets of observed $v$ data points | - |
| $\{q_i\}$ | Sets of all ranks for variable $q$ | - |
| $\{r_i\}$ | Sets of all ranks for variable $r$ | - |

## Parameters

| Symbol | Description | Unit |
|---|---|---|
| $b_0$ | Intercept of the regression line (constant term) | - |
| $b_1$ | Slope of the regression line | - |
| $n$ | Total number of samples | - |
| $\hat{\tau}$ | Kendall rank correlation coefficient | - |
| $n_t$ | The total number of concordant and discordant pairs in the sample | - |
| $n_c$ | The number of concordant pairs | - |
| $n_d$ | The number of discordant pairs | - |
| $C_{HCl}$ | Concentration of hydrochloric acid M | M(mol/L) |
| $m_{lignin}$ | Mass of lignin sample | g |
| $M_{NHND}$ | NHND molar mass | g/mol |

## Variables

| Symbol | Description | Unit |
|---|---|---|
| $x$ | Independent variable (predictor) | - |
| $\hat{y}$ | Estimate mean value of the response variable | - |
| $y_i$ | The experimental data points/observations | - |
| $\bar{y}$ | The mean value of the observations | - |
| $\hat{y}_i$ | The data points predicted by the model | - |
| $u_i$ | Measured value of variable $u$ | - |
| $v_i$ | Measured value of variable $v$ | - |
| $\bar{u}_.$ | Mean of $u$ values | - |
| $\bar{v}_.$ | Mean of $v$ values | - |
| $q_i$ | Rank of the $i$-th observation in variable $q$ | - |
| $r_i$ | Rank of the $i$-th observation in variable $r$ | - |
| $\bar{q}_.$ | Mean rank of $q$ values | - |
| $\bar{r}_.$ | Mean rank of $r$ values | - |
| $N[C_6H_5OH]$ | Number of phenol groups per gram of lignin. | mmol/g |
| $V_{B,HCl}$ | Total volume of HCl added at point B. | mL |
| $V_{A,HCl}$ | Total volume of HCl added at point A. | mL |
| $\frac{N[R-OH]}{g\ of\ lignin}$ | The number of OH groups per gram of lignin | mmol/g |
| $I_{OH}$ | Area under the NMR peak corresponding to phenolic OH | - |

| | | |
|---|---|---|
| $I_{NHND}$ | Area under the NMR peak of the internal standard (NHND) | - |
| $R$ | Integration ratio of the spectral region of interest ($I_{OH}$) over the internal standard region ($I_{NHND}$) | - |
| $m_{NHND}\ [g]$ | Mass of NHND used in the NMR sample | g |
| $RSA_{DPPH}$ | Radical scavenging activity against DPPH radicals | % |
| $RSA_{ABTS}$ | Radical scavenging activity against ABTS radicals | % |
| $ABS_{t=0}$ | Initial solution absorbance at time 0 | min |
| $ABS_{t=12\ min}$ | Solution absorbance after 12 minutes incubation | min |
| $ABS_{t=30\ min}$ | Solution absorbance after 30 minutes incubation | min |

# Contents

# List of Figures

# List of Tables

# 1

# Introduction

Lignin is one of the most generous gifts of nature, offering remarkable potential in various applications, including packaging[3], biofuels[4], and the food/biomedical industry[3] as an antioxidant. Lignin's benefits stem from its unique structural features. With strategic investment in studying lignin's structure and properties, this abundant byproduct can provide distinctive characteristics on an industrial scale.[5]

Lignin is a complex polymer and a key component of plant cell walls, playing a crucial role in plant strength, structure, and overall viability. It provides essential protection for plants against fungi, bacteria[6], UV light[7], and moisture[6]. These diverse properties arise from a complex chemical structure composed mainly of three cinnamic alcohols, which form a phenylpropanoid backbone.[6] These couplings involve various C–C and C–O bonds, such as β-aryl ether (β-O-4), with differing bond strengths.[6] Lignin is rich in functional groups, such as carboxyl, hydroxyl, carbonyl, and phenol groups, which can contribute to its unique properties, particularly its antioxidant activity.[8] However, the polyphenolic structure of lignin is widely regarded as the key contributor to its antioxidant activity since this structural characteristic is also observed in various antioxidants, such as vitamin E.[8], [9]

Antioxidants are crucial for protecting the body against oxidative stress, a condition that can arise from an imbalance between free radicals and the body's ability to neutralize them. Free radicals are highly reactive molecules with unpaired electrons that play a significant role in physiological processes. However, when their concentration becomes unbalanced due to environmental factors like UV radiation and heat, free radicals can trigger oxidative stress, increasing the risk of cardiovascular disease, cancer, and other health problems. These health conditions occur due to the reaction of the free radical with DNA bases, amino acid side chains in proteins, and double bonds in unsaturated fatty acids.[8], [10]

Antioxidants can react with free radicals by exchanging electrons and protecting against oxidative stress. They can either completely neutralize the free radicals or convert them to less harmful forms. The intake of antioxidants is significant for enhancing the body's natural defense system, which includes enzymatic activity, metal chelation, and scavenging of free radicals.[10] Therefore, studying natural antioxidants like lignin and utilizing their radical scavenging properties is of great importance. However, fully exploiting the potential of lignin, particularly as an antioxidant, presents several challenges.

Effective characterization of lignin, especially technical lignin obtained from industrial processes, remains a significant challenge. The monomeric construction of lignin varies in different plant species. Additionally, different extraction and purification processes lead to further variations in the lignin's structure.[6] Therefore, establishing a reliable structure-property relationship is essential for identifying the specific structural features that influence lignin's antioxidant properties. Conventional characterization methodologies only provide partial insight into the lignin's complex structure. For instance, phosphorous nuclear magnetic resonance spectroscopy, $^{31}$P NMR, can selectively identify hydroxyl groups on the lignin surface. However, factors such as high cost, complexity of the

methodology, toxicity of the reagents used, and concerns about stability and accuracy are limiting the effectiveness of this method.[11] To overcome these limitations, innovative and more efficient characterization techniques are needed.

It is crucial to identify functional groups and other elements in the lignin structure that are responsible for its antioxidant properties and determine the relative magnitude of their influence. Several studies indicated that lignin's antioxidant activity is due to its polyphenolic structure. Therefore, evaluating the impact of phenolic functional groups on lignin's antioxidant properties is of great importance.

## 1.1 Aim

This study aims to investigate whether the number of phenolic -OH groups is the dominant factor of antioxidant activity. To accomplish this objective, the project comprises three steps.

(1) To quantify phenolic-OH groups in various types of lignin using conductometric titration and $^{31}P$ NMR spectroscopy. It also allows for a comparison between these two methods in terms of accuracy, suitability, and precision.

(2) To measure the antioxidant activity in various types of lignin using DPPH (2,2-diphenyl-1-picrylhydrazyl) and ABTS (2,2′-azino-bis (3-ethylbenzothiazoline-6-sulfonic acid)) radical scavenging assays, and analyze whether there is a clear relation between antioxidant activity and the number of phenol-OH content.

(3) To look into the lignin structure and check for other structural properties that might influence antioxidant activity.

The results from these steps can provide data to investigate whether there is a direct correlation between the phenolic-OH group quantity and the antioxidant activity in the lignin.

# 2

# Theory

## 2.1 What is lignin

An introduction to the lignin structure

### 2.1.1 Lignin

Lignin is an abundant biopolymer in plant cell walls, providing strength and hydrophobicity for the lignocellulosic matrix.[6] Figure 1 illustrates lignin within lignocellulosic biomass. Lignin accounts for 15–30% of the mass fraction of lignocellulosic biomass.[3] It contributes to maintaining strength by protecting cellulose and hemicellulose and reducing biodegradation.[6] Importantly, lignin functions as a natural antioxidant protecting plant cells against oxidative stress.[5]

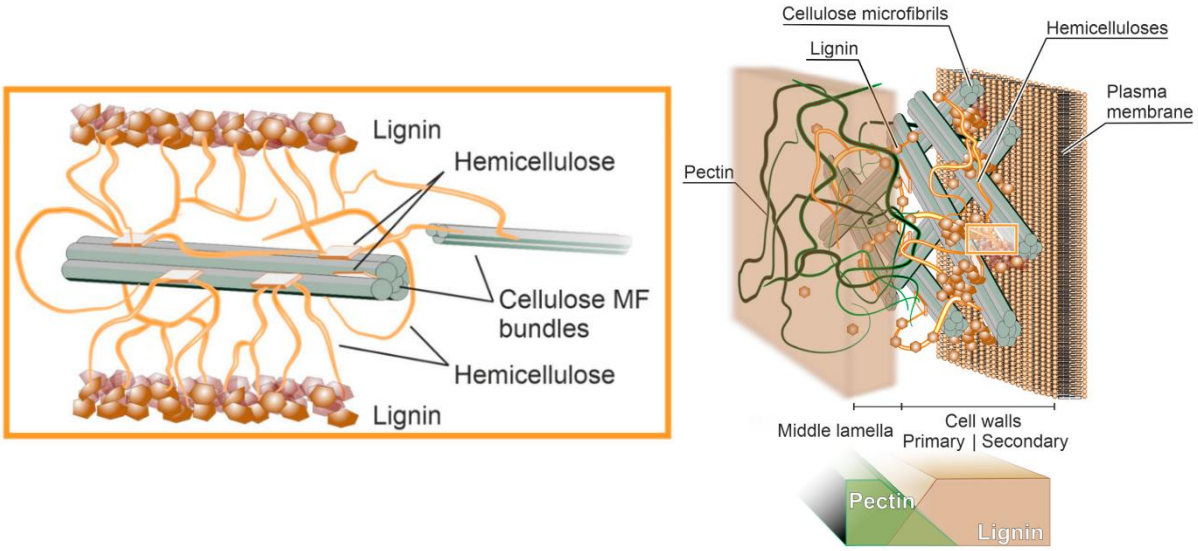


***Figure 1.*** *The complex and heterogeneous polymer structure of lignin within the secondary cell walls of plants. Figure reproduced from Balk et al. (2023) [13]*

### 2.1.2 Structure

Lignin has an aromatic structure composed of various functional groups and building blocks. Its structure is mainly composed of phenylpropane units, including three key cinnamic alcohols: sinapyl (3,5-dimethoxy-4-hydroxycinnamyl), coniferyl (3-methoxy-4-hydroxycinnamyl), and p-coumaryl alcohol (4-hydroxycinnamyl). These alcohols, also known as S-units, G-units, and H-units, form the

fundamental structures and build up phenylpropanoid groups, carbonyl groups (e.g., aldehyde, ketone, and carboxyl groups), and phenolic hydroxyl groups(phenolic-OH).[3] The radical coupling between these phenylpropane units occurs by various C-C and C-O linkages with different bond dissociation energies (BDE). Some of these crosslinking molecules are β-aryl ether (β-O-4), α-aryl ether (α-O-4), 1,2-diaryl propone (β-1), phenyl coumaran (β-5), biphenyl (5–5, α-1), and diphenyl ether (5-O-4). Figure 2 presents the chemical structure of softwood kraft lignin. The β-O-4 bond exhibits the lowest BDE of all lignin linkages, making it the most susceptible to cleavage. This cleavage generates new aromatic hydroxyl groups, including phenolic hydroxyls, which can potentially enhance antioxidant activity by increasing the phenolic content.[3]

Chromophores are regions in lignin's structure that are associated with UV absorption properties and color variations.[7], [14] The chromophore components in lignin are mainly structures related to quinoids, catechols, aromatic ketones, stilbenes, and conjugated carbonyls with phenolics. Also, additional chromophores might be generated through oxidation or during the pulping process.[7] These structures are rich in conjugated functional groups. The conjugated double bonds can stabilize the phenolic radical formed after free-radical neutralization, so-called phenoxyl radical (Ar–O•), by resonance delocalization and stereoelectronic effects.[14]

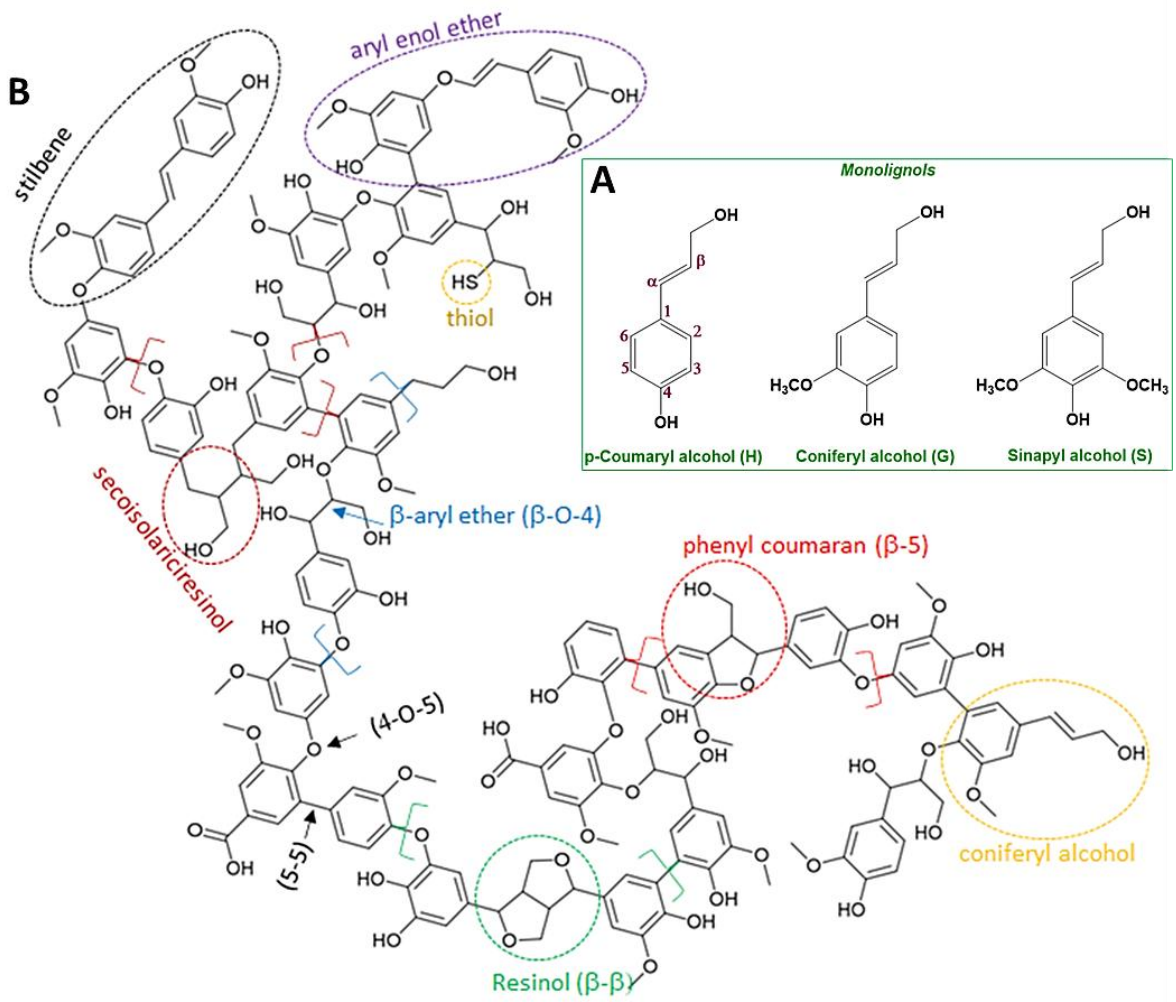


***Figure 2.*** *(A) Chemical structures of three key cinnamic alcohols in the lignin structure: p-coumaryl alcohol (4-hydroxycinnamyl), coniferyl (3-methoxy-4-hydroxycinnamyl), and Sinapyl (3,5-dimethoxy-4-hydroxycinnamyl).* ***(B)*** *Structure of Monolignols (A) and softwood Kraft lignin (B), reproduced with permission from Crestini, C, et al [15] courtsy of Ahilan Manisekaran.*

### 2.1.3 Species-based variations in lignin structure

The structure of the lignin varies between plant species. Softwood plants, such as fir, pine, and spruce, are gymnosperms and originate from coniferous trees. Hardwood plants, such as oaks, maples, and birches, are angiosperms and originate from deciduous trees.[6] Based on this classification, the lignocellulosic biomass also divides into softwood and hardwood. Additionally, a third category of lignocellulosic biomass originates from annual grasses.[6], [8]

The weight percentage of lignin content varies in different biomass categories. The lignin content constitutes 30 wt.% in softwood, 20-25 wt.% in hardwood, and 10–15 wt.% in grass-based wood biomass.[8] Additionally, the monomeric structure of lignin varies in different plant species. In hardwoods, Lignin mainly contains S-units (50–75%) and G-units (25–50%), with a low number of H-units. In softwoods, almost all the lignin consists of G-units (90–95%), with very few S-units (0–1%) and a small percentage of H-units (0.5–3.4%). Grasses have a mix, with 25–50% G-units, 25–50% S-units, and 10–25% H-units.[5]

## 2.2 Lignin types

## Industrial-based variations in the lignin structure, processing techniques, and common modifications

### 2.2.1 Lignin's current place in industry and potential

The original form of lignin, which exists in lignocellulosic biomass, is not directly available, as it undergoes structural modifications during the extraction process. Lignin is produced in large quantities as a by-product in pulp and paper industries, referred to as technical lignin.[16] Lignin holds significant potential across a range of applications due to its unique characteristics and its availability. The application of lignin in food packaging has been shown to enhance UV protection, anti-oxidation, and protection against oxygen.[17] The strong and stable structure of lignin can improve the mechanical strength and thermostability of polymer materials.[7] Introducing plastic materials with lignin-based macromolecules (e.g., as a reinforcement/blend) can reduce their environmental carbon footprint.[18] Due to its higher energy and carbon content per mass compared to other bio polymers such as cellulose, lignin is a good candidate as a biofuel source.[19] Due to its UV-absorbing and oxidation-resistant properties, Lignin's application as a natural ingredient in sunscreen products is under investigation.[20] Several techniques have been developed for lignin separation and recovery from the pulping products for various applications.

### 2.2.2 Industrial-based variations in lignin structure

Lignin is a heterogeneous polymer that exists in various types. These differences arise from variations in its molecular structure and size, which are influenced not only by the plant species but also by various industrial processes. Lignin undergoes slight structural changes during different processing steps and techniques in the paper industry. Lignin is isolated from wood through various pulping methods, including the Kraft, Soda, and Organosolv processes.[6]

#### 2.2.2.1 Kraft pulping

Currently, Kraft pulping (Figure 3) accounts for 90% of the produced chemical pulp worldwide. It is responsible for a significant portion of the lignin produced, known as kraft lignin. Kraft pulping induces fragmentation and dissolution of lignin through a series of chemical reactions and leads to the cleavage of the β-O-4' alkyl-aryl ether bonds in its structure. In some cases, the monomeric or oligomeric lignin

fragments released from this process can undergo radical redox reactions, leading to recondensation processes and fragmentation, and reduction processes. Nevertheless, the Kraft process offers valuable advantages, including a high quantity of the initial product and relatively low production cost.[21] After the pulping process, lignin can be extracted from the pulp mill using several techniques. It can either be recovered as crude black liquor or extracted by precipitation. LignoForce® and LignoBoost® are some examples of industrial extraction technologies to obtain high-purity lignin from black liquor. These methods extract lignin by decreasing its solubility in the liquor through acidification, followed by lignin separation via filtration.[21]

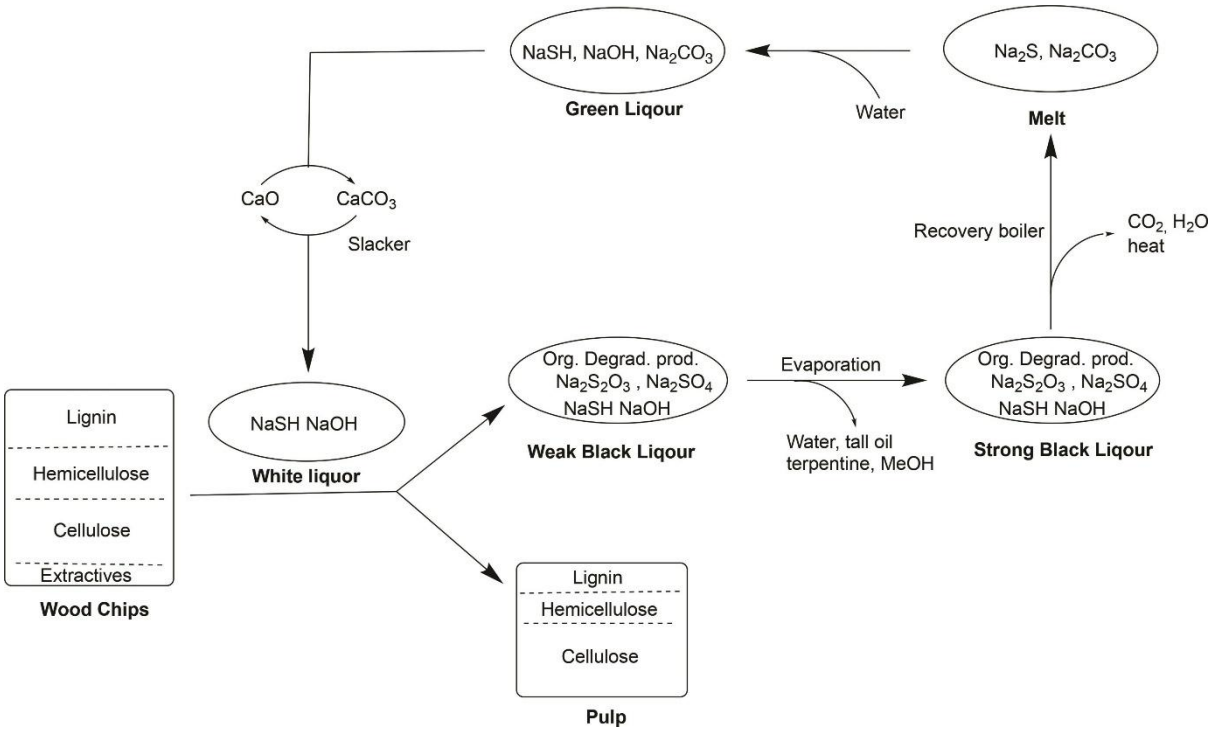


***Figure 3.*** *A picture of the Kraft process. Adopted with permission from Ref.[21]*

The LignoBoost® extraction process consists of two main procedures: precipitation and filtration. The precipitation step occurs by acidifying black liquor (with about 40% dry substance) using carbon dioxide. During this step, lignin's phenolic compounds will be protonated and precipitated as solid particles. The resulting slurry is filtered by a filter press, yielding a solid composed of moist lignin with high ash content. The ash content is separated by acidic washing with sulfuric acid (pH 2-3)[22], resulting in the production of lignin with high purity and less than 1% of ash. A final filtration step separates the final lignin product, which has a 35% moisture content. Figure 4a illustrates the LignoBoost® process. This technique has been applied in two commercial plant companies so far: Stora Enso's Sunila mill in Finland, with a demonstration plant also operating in Bäckhammar, Sweden, and Domtar's Plymouth mill in North Carolina, USA.[21]

The LignoForce® process is like the LignoBoost® process with some minor modifications (Figure 4b). This process is relatively simple and can reduce toxic $H_2S$ emissions. Briefly, the LignoForce® process starts with the oxidation of black liquor, which alters the particle-forming behavior of lignin. This alteration eliminates the additional filtration steps performed in the LignoBoost® process. In this extraction, the filtration occurs during a single filter press**,** which also includes washing and protonation of lignin with sulfuric acid. Despite this, the final lignin will have similar characteristics to LignoBoost® lignin.[21] According to Maria Juliane Suota et al.[6], softwood LignoForce® lignin has

higher total OH content, lower β-O-4′, and higher molecular weight ($M_w$) than hardwood lignin. While hardwood Lignin is less condensed, more soluble, and less stable than softwood Lignin.[6]

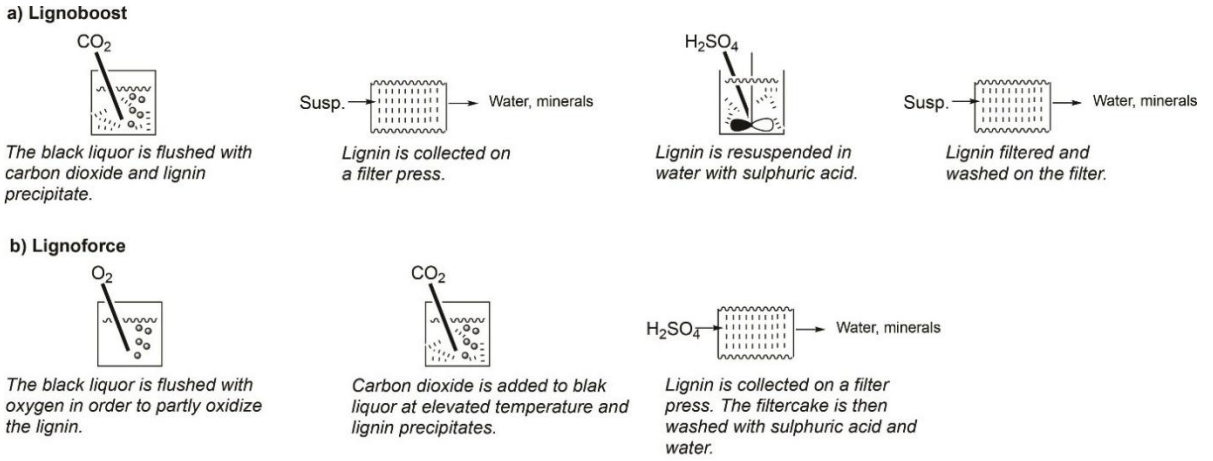


***Figure 4.*** *A picture of a) LignoBoost®; and b) LignoForce® lignin recovering techniques. Adapted with permission from Ref [21]*

#### 2.2.2.2 Organosolv pulping

Organosolv processing uses organic solvents to extract lignin, the extracted lignin is known as Organosolv lignin. Organosolv extraction techniques can be an alternative to the kraft process. Similar to Kraft pulping, the breakage of ether bonds leads to the formation of new phenol groups.[23], [24] The lignin product from the Organosolv process is highly phenolic, relatively hydrophobic, and less contaminated. Compared to Kraft lignin, it has a lower molecular weight and higher purity (less ash content, and carbohydrate content).[24] This process is also free of sulfur. However, this process is not cost-effective and thus not suitable for industrial scale.[24]

### 2.2.3 Lignin modifications

Although lignin has a lot of potential, the practical utilization of this material has limitations due to its complicated chemical structure, thermal instability, and low reactivity.[25] Modification of the lignin is typically performed with the aim of improving or adding specific characteristics to this component, which in turn enables its use in various applications. These improvements can include reactivity, solubility, blending, and composite making. Lignin modifications can be performed through different mechanisms. Some of the examples are alkylation, esterification, etherification, phenolation, and urethanization.[12] In this study, we used aminated and hydroxy-ethylated lignin, produced by Liyang Liu et.al.

### 2.2.3.1 Etherified lignin derivatives (HEOSHL & HESKL1)

Hydroxy-ethylated (HE) softwood kraft lignin (SKL1) and organosolv hardwood lignin (OSHL) were produced through a green process by Liu et al.[26] An excess amount of ethylene carbonate (8 g), abbreviated as EC, was mixed with 5 g dried lignin powders with a molar ratio equal to EC/(ArOH + COOH) = 6.6 . The reaction was performed in a 50 ml round-bottom flask at 80 –120 °C for 0–6 h. The flask was sealed with a rubber-septa, Teflon film, and parafilm to avoid leakage. The $CO_2$ gas was collected using a self-designed analytical equipment and recorded as a function of time.[26] This modification replaces phenolic -OH groups with aliphatic -OH groups in OSHL and SKL, forming of HESKL1 and HEOSHL. For the HESKL1, the weight-average molecular weight (Mw) was 278.5 kDa, corresponding to 86 mL/g $CO_2$ released during the reaction, and the degree of substitution (DS) were 88%.[26] These numbers were 14.9 kDa Respective 91% for the HEOSHL lignin.[27] Figure 5 briefly presents the reaction mechanism of HE-modification.

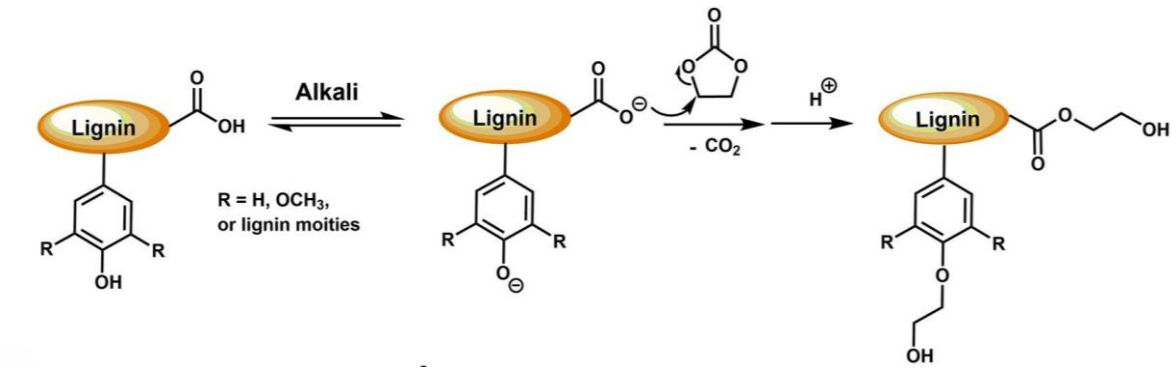


***Figure 5.*** *Reaction scheme of green Hydroxy-ethylating process using ethylene carbonate. Adopted from Ref.[26]*

### 2.3.3.2 Aminated lignin (Amine SKL3)

Liu et al.'s aminated lignin building blocks are produced from the softwood kraft Lignin. The resulting lignin demonstrated enhanced reactivity and altered solubility. During this process, the 2-oxazolidinone (OZD) was used as a solvent and reagent, and the modification was performed for 2-4 hours at 150 °C in the presence of an alkaline catalyst (NaOH) (Figure 6). During the reaction, the deprotonated ArOH and COOH groups in lignin were selectively modified by the OZD. This process leads to the formation of primary amine groups from aminoethylation or secondary amine groups arising from urea-linked hydroxyethyl groups. (DS= 66% and Molecular Weight ($M_n$) = 9.0 kDa) More specifically, this process leads to the replacement of phenolic -OH groups with amine groups, resulting in the creation of Aminated building blocks from softwood kraft lignin.[25]

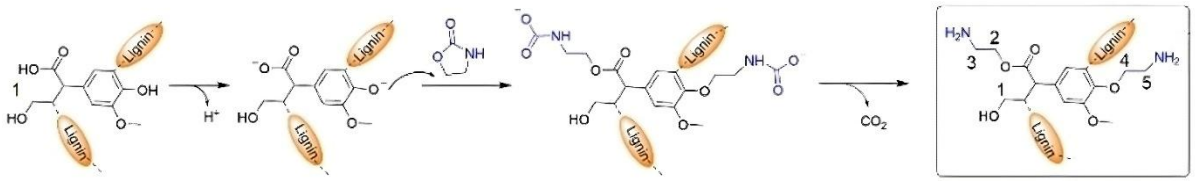


***Figure 6.*** *Reaction scheme of green animation process using 2-oxazolidinone (OZD). Adopted from Ref.[25]*

### 2.2.4 Lignins studied in this project

Seven lignin variants were investigated in this study. The selected lignins represent diverse categories based on species origin (e.g., hardwood, softwood), processing methods (e.g., LignoBoost®, LignoForce®), and chemical modifications (i.e., native and modified forms).

A brief description of each lignin variant is provided below.

**Organosolv hardwood lignin (OSHL)** is kindly donated by our collaborators at Suzano (Brazil). It is extracted from Eucalyptus trees using ethanol/water with acidic catalysis.

**Softwood kraft lignin 1 (SKL1)** is provided by Domtar Corp. (US). This lignin is isolated from black liquor generated in the Kraft pulping process via the LignoBoost® method. This lignin usually has the lowest ash content compared with other lignin resources.

**Softwood kraft lignin 2 (SKL2)** is another kind of alkali lignin from Ingevity Corporation (US, South Carolina). This lignin was also extracted from black liquor produced during Kraft pulping process. The raw wood materials are softwood, but the purification process is slightly different from the LignoBoost® process.

**Softwood kraft lignin 3 (SKL3)** is isolated from black liquor via the LignoForce® process. This lignin is kindly donated by WestFraser (Canada, Alberta). Unlike SKL1 and SKL2, this lignin contains a significant amount of acidity, requiring an additional washing procedure before characterization.

**Hydroxyethyl softwood kraft lignin (HESKL1)** is acquired by modifying SKL1 using ethylene carbonate. Previous studies have described the modification methods.[26] This ethylene carbonate can selectively functionalize the phenol and carboxylic acid groups on the lignin surface, leaving primary aliphatic OH groups. After the modification, lignin is quite difficult to dissolve in organic solvents and aqueous alkali, except DMSO.

**Hydroxyethyl hardwood organosolv lignin (HEOSHL)** is obtained by a similar modification to the HESKL1 methods with slightly different conditions. The organosolv hardwood lignin is used as a raw material, resulting in products that usually have good solubility in organic solvents than HESKL1.

**Aminated softwood kraft lignin (Amine SKL3)** is acquired by modifying SKL3 using OZD.[25] The OZD can selectively convert phenol groups on the lignin surface into amine groups, associated with an increase in molar mass and changes in solubility parameters. As such, the aminated lignin has difficulty dissolving organic solvents and aqueous alkali, except in DMSO.

**Table 1.** Presents the abbreviations used for the investigated lignin in this study.

| | |
|---|---|
| Hardwood organosolv lignin | OSHL |
| Softwood kraft lignin 1 | SKL1 |
| Softwood kraft lignin 2 | SKL2 |
| Softwood kraft lignin 3 | SKL3 |
| Hydroxyethyl hardwood organosolv lignin | HEOSHL |
| Hydroxyethyl softwood kraft lignin | HESKL1 |
| Aminated softwood kraft lignin | Amine SKL3 |

# 2.3 Antioxidant activity of lignin

## An insight into lignin's antioxidant activity, structural impact, and limitations

### 2.3.1 Antioxidant activity

The antioxidant characteristic refers to the ability of a substance to protect cells from damage caused by free radicals.[9] This protection occurs by preventing the oxidation of molecules through scavenging free radicals. Free radicals are molecules with one or more unpaired electrons, which prompts them to stabilize themselves by reacting with other molecules. Factors such as high temperature, oxidants, or ionizing radiation caused by UV light can lead to the formation of free radicals.[8], [9]

Figure 7 provides a brief overview of intracellular oxidative stress, its consequences, and the role of antioxidants in preventing it. Free radicals accumulate excessively when the production of reactive oxygen species (ROS) is imbalanced due to the above-mentioned factors. ROS refers to a group of oxygen-containing molecules generated during physiological processes. An imbalance in the production rate of ROS can result in oxidative stress, leading to the formation of various free radicals, including peroxyl (ROO•) and hydroxyl(•OH) radicals. These molecules are highly reactive and unstable at room temperature. Excessive ROS can react with cell membranes, DNA, and other biomolecules, leading to protein degeneration, lipid peroxidation, and cell death.[8] These unwanted reactions can lead to rapid aging and cancer.[8], [9]

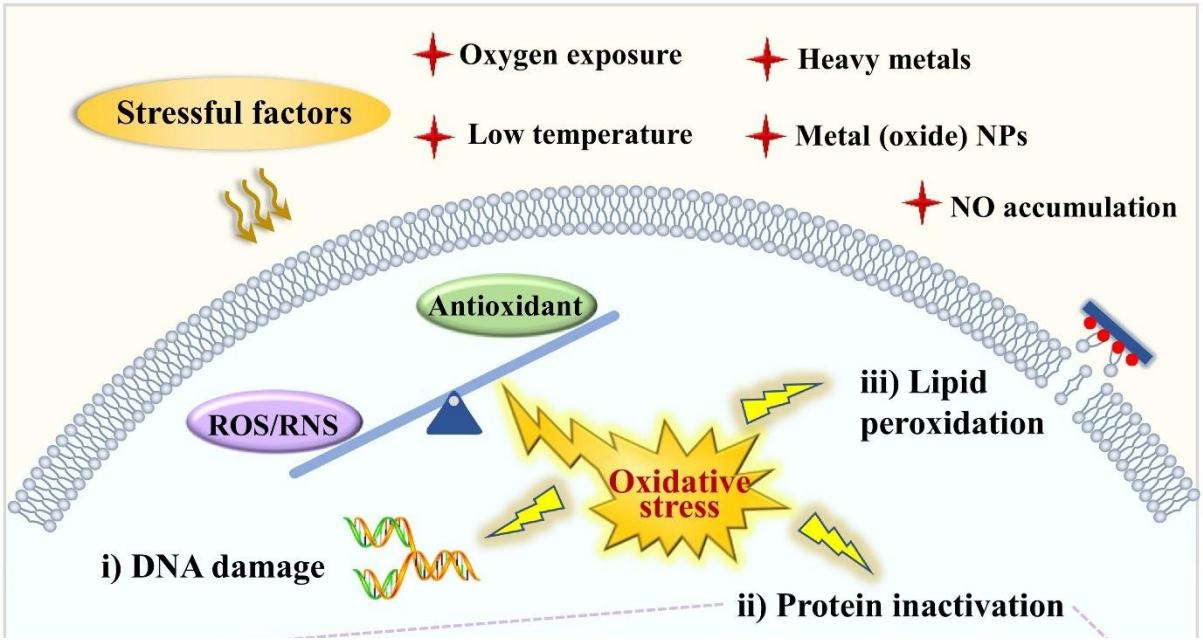


***Figure 7.*** *Intracellular imbalance between ROS (reactive oxygen species) and antioxidant concentrations and its consequences. Adopted from Ref.[28]*

The efficacy of antioxidants depends on various factors, such as chemical structure, concentration, and the antioxidant reactivity with ROS.[29] Antioxidants can be natural or synthetic.[8] Natural antioxidants refer to the antioxidants that exist in fruits and vegetables, including vitamin C, tocopherols, carotenoids, and flavonoids. Synthetic antioxidants are developed in laboratories.

Examples of synthetic antioxidants include butylated hydroxyanisole (BHA), butylated hydroxytoluene (BHT), propyl gallate (PG), and tert-butyl hydroquinone (TBHQ).[8]

Although synthetic antioxidants have optimal antioxidant properties, they have some limitations and drawbacks. The production of synthetic antioxidants is costly. Some synthetic antioxidants, such as BHA and BHT, are cytotoxic and carcinogenic.[8] Additionally, they can lead to greater side effects compared to natural antioxidants.[8] Reports about PG demonstrate that it can induce mutagenesis, which in turn can lead to DNA damage and also accelerate aging. Natural antioxidants, on the other hand, are more suitable for human consumption and can be derived from existing natural resources.[8] Lignin, a byproduct already produced in excess in the paper industry, is an excellent example of a nature-derived antioxidant.

### 2.3.2 Lignin as an antioxidant

Lignin offers antioxidant properties and can scavenge free radicals.[29] During plant growth, the massive polymeric structure of lignin protects plants against any biological, chemical, and mechanical stresses. Neutralizing these harmful free radicals reduces cellular damage.[8] A study by Rumpf et al. on lignins from Paulownia and Silphium showed that these lignins possess great antioxidant activity and have potential to be used as additives in food packaging or for biomedical applications.[29] Azadfar et al. demonstrates that the antioxidant capability of lignin is comparable to commercial antioxidants, guaiacol, and butylated hydroxytoluene.[30]

There is a general belief that the antioxidant properties of lignin are primarily due to the presence of excess phenolic compounds and other oxygen-containing functional groups in its structure.[12] They include aliphatic hydroxyl, carbonyl, and carboxyl groups. Particularly, the phenolics can form quinomethides, a common characteristic shared with many other antioxidants such as polyphenols, phenolic acids, and vitamins.[8], [9]

The polyphenolic structure of lignin reportedly prevents oxidative stress and excess ROS in several ways. The phenolic hydroxyl groups (Ar-OH) in lignin allow it to scavenge the free radicals (R •) through hydrogen atom transfer (HAT) and single electron transfer (SET) reactions (Scheme 1).[12] They can protect molecules against factors that provoke ROS production, such as light exposure and radiation. Additionally, the phenolic groups can generate less reactive, partially oxidized free radicals instead of highly reactive and harmful ones.[8] According to reports, lignin's antioxidant activity varies with the availability of phenolic hydroxyl groups and their stability.[8]

**ArO–H + R • → ArO • + R–H** [12]

Scheme 1. Radical scavenging mechanism of Phenol hydroxyl groups

The stability of phenoxy radicals arises from structural features. An example is ortho-substituents (methoxy groups) in lignin, which stabilize (ArO•) through resonance and improve antioxidant activity. In addition, the π-π system in lignin increases the stability of the generated free radicals by enabling the delocalization of unpaired electrons. Conjugated double bonds also stabilize phenoxy radicals through extended delocalization, and conjugated carbonyl groups have little effect on antioxidant activity.[8]

In addition to functional groups and structural characteristics, other factors such as molecular weight, polydispersity, biomass source, extraction method, and post-treatments can influence antioxidant.[12] For instance, Kaur et al. demonstrated that unmodified lignin from sugarcane bagasse had

higher antioxidant activity than its chemically modified version by acetylation and epoxidation.[12] Wang et al. proposed that the antioxidant activity of enzymatic hydrolysis lignin fractions increases as their molecular weight decreases.[31]

Various assays can be employed to measure lignin's antioxidant activity, including chemical assays with specific reagents and cell-based assays.[29]

### 2.3.3 Antioxidant activity measurement

Antioxidant assays can be categorized based on the reaction mechanism: Hydrogen atom transfer (HAT) or single electron transfer (SET).[8], [29] SET mechanism refers to the transfer of a single electron from antioxidants to free radicals, protecting other compounds from reacting with them.[8] HAT, on the other hand, refers to the donation of hydrogen atoms from antioxidants and the transfer of one bonding electron between protons to neutralize free radicals. However, in practice, the antioxidant activity can occur through more complicated mechanisms, such as mixed HAT/SET, stepwise electron transfer-proton transfer, concerted electron–proton transfer, or sequential proton loss electron transfer (SPLET).[8], [29] It is reported that the antioxidant mechanisms in lignin are the HAT, SPLET, and proton-coupled electron transfer (PCET). PCET mechanism refers to the transfer of both protons and multiple electrons. In the HAT mechanism, electron transfer occurs to a single radical orbital, while in PCET, multiple molecular orbitals are involved.[8]

The DPPH (2,2-diphenyl-1-picrylhydrazyl) and ABTS (2,2′-azino-bis (3-ethylbenzothiazoline-6-sulfonic acid)) assays are widely used chemical-based analytical methods for quantifying radical-scavenging activity. DPPH and ABTS molecules act like a stable free radical with a reactive electron after activation with a solvent. The effectiveness of lignin neutralizing these stable free radicals (DPPH, ABTS) can be represented as radical scavenging activity (RSA). RSA is the amount of free radicals (DPPH and ABTS) neutralized by lignin, which is expressed as a percentage. Both assays follow HAT and SET mechanisms. It is important to note that DPPH is suitable for hydrophobic antioxidants, while ABTS is suitable for both hydrophilic and hydrophobic antioxidants.[8]

In the DPPH assay, the DPPH free radical solution has a purple color due to the delocalization of excess electrons on the molecule, which has a distinct absorption peak at 515-520 nm in UV-Vis spectrophotometer measurements. Addition of an antioxidant leads to the neutralization of DPPH since the antioxidant’s hydrogen ions react with DPPH. Depending on the strength of the antioxidant, the intensity of the absorption peak decreases and the solution color changes toward yellow (Figure 8). The antioxidant capacity of an antioxidant can be determined by measuring the initial absorbance of the DPPH solution and the final absorbance of the mixture after the addition of the antioxidant. The difference between these two absorptions divided by the initial absorbance, in percent, shows the radical scavenging activity. In other words, the RSA shows the percentage of neutralized DPPH radicals. The formula used to calculate RSA_DPPH is provided in the Materials and Methods section (Section 3.4).[8]

The DPPH assay is simple, rapid and inexpensive and is suitable for solid, liquid and biological samples. However, the DPPH molecule’s steric hindrance, stability, visible light exposure, concentration, and reaction time may influence the RSA measurement.[8]

In the ABTS assay, the $ABTS^+$ free radical solution is produced by reacting with potassium persulfate ($K_2S_2O_8$), forming dark blue-green solution through oxidation reaction. This solution has a distinct absorption at three points: 660, 734, and 820 nm. Among these peaks, the absorbance at 734 nm is generally considered and measured to avoid other interferences. After the addition of the antioxidant and neutralization of $ABTS^+$ free radicals with hydrogen ions, the peak intensity at 734 will be decreased, and the solution's color becomes lighter (Figure 8). The RSA in this methodology is determined similar to the DPPH assay. The formula used to calculate RSA_ABTS is provided in the Materials and Methods section (Section 3.5).[8]An advantage of the ABTS assay is the longer lifetime of the radical compared to hydroxyl radical, and oxygen ion radical. This method doesn't require high temperature to produce free radicals and can study antioxidant activity over a wide pH range. This can avoid interference from endogenous peroxidase activity and make the determination of the antioxidant activity of amphiphilic substances more accurate.[8] The chemical structure of DPPH and ABTS and the reaction mechanism with antioxidants are presented in Figure 8.

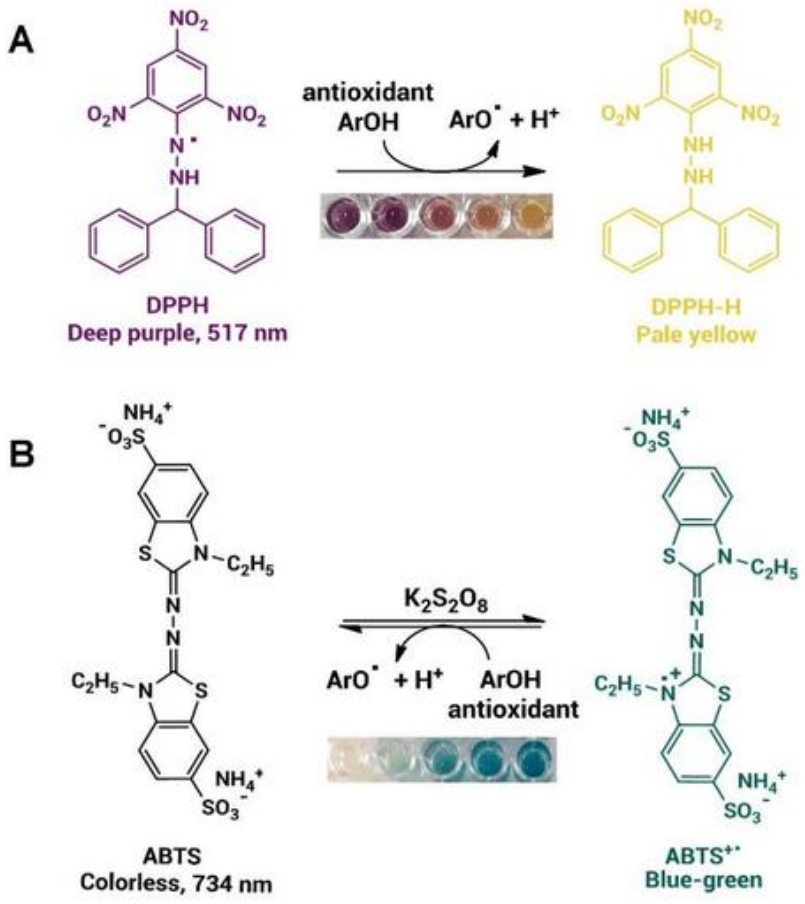


***Figure 8.*** *Reaction mechanism of (A) DPPH(2,2-diphenyl-1-picrylhydrazyl) and (B) ABTS (2,2'-azino-bis (3-ethylbenzothiazoline-6-sulfonic acid)) assays. Adapted from ref.[32]*

### 2.3.4 Limitations and challenges

Although lignin has considerable antioxidant properties, its practical application is limited by several challenges, both in antioxidant packaging materials and in biomedicine.

Studying antioxidant activity is complicated in general, since no single methodology can fully capture how a possible antioxidant would function in vivo.[29] When it comes to lignin, its variety and complex structure further complicate the determination of specific chemical structures that lead to the antioxidant

activity, compared to other polyphenols such as flavonoids and tannins.[8] The heterogeneity of lignin in its natural form is also challenging for developing and applying this polymer for biomedical purposes.[12] There is insufficient understanding of the mechanism of lignin breakdown by the human body.[12] In vivo effects of lignin as an anti-oxidants should be investigated to bring it to actual application.

In polymer applications, technical lignin have poor miscibility with numerous polymer matrices. Thus, chemically modified lignins were developed.[33] The antioxidant properties remain intact in lignin-based copolymers. An example is lignin–poly (ε-caprolactone-co-lactide), produced by Dan Kai et. al.[34], reported to exhibit good antioxidant activity. In conclusion, application of lignin as an antioxidant requires a directed study of its structure and its correlation with antioxidant activity.

## 2.4 Correlation statistical analysis

Correlation analyses are useful to investigate the influence of a specific quantitative variable on another variable. More specifically, when the value of one variable increases, the value of another tends to increase or decrease, can be defined as how correlated the two variables are. Additionally, the intensity and direction of this correlation can be determined through various correlation tests.[35]

This research aims to investigate the correlation status between antioxidant activity and the number of phenol groups in lignin. We mainly performed linear regression analysis. Additionally, Pearson analysis, Spearman analysis and Kendall's Tau analysis were performed to validate the results from linear regression.

### 2.4.1 Linear regression analysis

A simple approach is to plot the data in a scatter plot and fit a regression linear trendline to the data points. The equation for the linear trendline is as follows:

$$\hat{y} = b_0 + b_1 x \tag{1}$$

In equation 1, $\hat{y}$ is an estimate mean value of the response variable, $b_0$ is the y-intercept, and $b_1$ is the slope, and $x$ is the predictor variable.

After fitting a trendline to the data points, the next step is to determine how well the data is fit to the trendline, and thereby how well the two variables are related. This can be determined by the analysis of variance and calculating the Coefficient of determination ($R^2$). To achieve this, the total variation in the data is divided into two parts: the variation explained by the regression line and the variation that is left unexplained as random error. These are calculated using sums of squares. As a result, the total variability in the sample measurements (SST) equals the variability explained by the regression line (SST) plus the sums of squares for error (SSE). Equation 3 shows how these three sum of squares are calculated.

$$SST = SSR + SSE \tag{2}$$

$$\sum(y_i - \bar{y})^2 = \sum(\hat{y}_i - \bar{y})^2 + \sum(y_i - \hat{y})^2 \tag{3}$$

In this equation the $y_i$ is the experimental data points (e.g. phenolic content/the antioxidant activity of a lignin sample), The $\bar{y}$ is the mean value of the observations (mean phenolic content or mean antioxidant activity across all samples), and $\hat{y}_i$ is the data points predicted by the model. In other words,

the SSR is the explained variation of the data points by the model, and the SSE is the unexplained variation of the model.

From these sums of squares, the $R^2$ can be calculated as follows.

$$R^2 = \frac{Explained\ variation}{Total\ variation} = \frac{SSR}{SST} = 1 - \frac{SSE}{SST} \quad (4)$$

The Coefficient of Determination measures the percentage of variation in the response variable (y) explained by the model. Values range from 0 to 1, with values close to 0 will worse fit and values close to 1, indicating very good fit.[36] Table 2 visualizes the model fit for different $R^2$ values.

**Table 2**. Interpretation of model fits based on the coefficient of determination ($R^2$). Adapted from ref.*[37]*

| $R^2$ | Interpretation |
|---|---|
| 0.00-0.199 | Very weak |
| 0.20-0.399 | Weak |
| 0.40-0.599 | Medium |
| 0.60-0.799 | Strong |
| 0.80-1.00 | Very strong |

Linear regression analyses were performed in Google Colab using the linregress function, following the general command:

slope, intercept, r_value, p_value, std_err = linregress (x, y)

r_squared = r_value ** 2

Where x and y represent the independent and dependent variables, respectively. The resulting outputs include the slope, intercept, correlation coefficient (r_value), significance level (p_value), and standard error (std_err). R2 is calculated as the square of the correlation coefficient. A detailed example of the full analysis code and the plotting is provided in Appendix A.

### 2.4.2 Pearson analysis

Pearson's product-moment correlation coefficient, or Pearson's *r*, is the most widely used technique for correlation analysis. This technique requires that both variables are normally distributed and there is a linear relationship between them. When these requirements are not fulfilled, it can lead to errors in the conclusion.[35]

For a total amount of n samples and two measured continuous variables, $u_i$ and $v_i$ within the sample ($1 \leq i \leq n$), the Pearson's $r(\hat{\rho})$ is calculated as follows.[38]

$$\hat{\rho} = \frac{\sum_{j=1}^{n}(u_i - \bar{u}_.)(v_i - \bar{v}_.)}{\sqrt{\sum_{i=1}^{n}(u_i - \bar{u}_.)^2}\sqrt{\sum_{i=1}^{n}(v_i - \bar{v}_.)^2}} \quad (5)$$

$$\bar{u}_{.=} \frac{1}{n}\sum_{i=1}^{n} u_i\,,\ \bar{v}_{.=} \frac{1}{n}\sum_{i=1}^{n} v_i \quad (6)$$

where $\bar{u}.$ and $\bar{v}.$ are the means of $u_i$respective $v_i$data points. The Pearson correlation $\hat{\rho}$ ranges between -1 and 1, in which 1 shows a perfect positive correlation, -1 shows a perfect negative correlation, and 0 shows no correlation between the variables.[38]

Pearson correlation analysis was performed in Excel using the general form of the commands =CORREL(array1; array2) or =PEARSON(array1; array2), where array1 and array2 represent the ranges of cells containing the two variables of interest.

### 2.4.3 Spearman analysis

For cases in which the normal distribution is not fulfilled, the Spearman rank order correlation coefficient (ρ) substitutes the original data for their ordered ranks. It doesn't require linear relationship between variables, as long as they exhibit monotonic behavior. In other words, they must exhibit a gradual relationship in the same direction (rising or falling) for the whole domain of the data studied.[35]

Let $q_i$ ($r_i$) denote the rankings of $u_i$ ($v_i$), ($1 \leq i \leq n$). Spearman's ρ is defined as:

$$\hat{\rho} = \frac{\sum_{j=1}^{n}(q_i - \bar{q}.)(r_i - \bar{r}.)}{\sqrt{\sum_{i=1}^{n}(q_i - \bar{q}.)^2}\sqrt{\sum_{i=1}^{n}(r_i - \bar{r}.)^2}} \tag{7}$$

$$\bar{q}.= \frac{1}{n}\sum_{i=1}^{n} q_i \, , \bar{r}.= \frac{1}{n}\sum_{i=1}^{n} r_i \tag{8}$$

Whereas $q_i$and $r_i$ are the rankings of the original variables $u_i$and $v_i$. The ranking refers to the order of the variables. What is $\bar{q}.$ and $\bar{r}.$.The Spearman $\hat{\rho}$ ranges between -1 and 1, in which 1 shows a perfect positive correlation, -1 shows a perfect negative correlation, and 0 shows no correlation between the variables $u_i$ and $v_i$.[38]

In other words, $\hat{\rho}$ equal to 1 means that both variables have the same ranking *(*$q_i = r_i$), and thereby.

$$u_i < u_j, v_i < v_j \; or \; u_i > u_j, v_i > v_j \; for \; all \; 1 \leq i < j \leq n$$

It means that whenever one observation has a higher (or lower) rank in u, it also has a similar higher (or lower) rank in $v$.

Any two sets of variables that follow the relationship above are concordant.

In contrast, $\hat{\rho}$ equal to -1 means that variables have a perfect negative correlation ( $q_i = n - r_i + 1$), which means that whenever one observation has a higher rank in u, it has lower rank in $v$ and vice versa.

$$u_i < u_j, v_i > v_j \; or \; u_i > u_j, v_i < v_j \; for \; all \; 1 \leq i < j \leq n$$

Any two sets of variables that follow the relationship above are discordant.[38]

Spearman correlation analysis was performed in Excel using the general form of the commands =CORREL(array1; array2) applied to the rank of the data. In other words, array1 and array2 in this case correspond to the ranges of cells containing the ranked values of the two variables.

### 2.4.4 Kendall's Tau analysis

Another alternative for the not-normally distributed data, is the Kendall's rank correlation coefficient (*Tau*-b), which substitutes the original data for their ordered ranks. It doesn't require linear relationship

between variables, as long as they exhibit monotonic behavior. The Kendall's Tau-b coefficient (τ or $t_b$) is robust to extreme data (outliers), giving it a greater capacity for populational inference and a smaller estimation error.[35]

Similar to Spearman's ρ, Kendall's Tau also implies the concepts of concordance and discordance to access the correlation between two variables. However, this methodology uses the notion of concordant and discordant pairs directly in the definition of this correlation measure. Specifically, Kendall's $\tau$ (sample version) is calculated through Equation 9.

$$\hat{\tau} = \frac{n_c - n_d}{n_t} \tag{9}$$

$$n_t = \frac{1}{2} n(n-1) = n_c + n_d \tag{10}$$

$$n_c = number\ of\ concordant\ pairs$$
$$n_d = number\ of\ discordant\ pairs$$

Where $n_t$ is the total number of concordant and discordant pairs in the sample. $\hat{\tau}$ varies between -1 and 1, with -1 corresponding to the perfect discordance, 0 indicating no association between the variables, and 1 corresponding to the perfect concordance.[38]

Kendall's Tau correlation analysis was performed using Equations 9 and 10 (see Appendix B for a detailed example of the calculation).

# 3

# Materials and Methods

To investigate potential correlations between lignin structure and antioxidant activity, a range of analytical techniques was applied to seven different lignin types. However, incomplete dissolution of some samples in the selected interfered with the accuracy of the measurements. As a result, the modified lignins—Amine SKL3, HEOSHL, and HESKL1—were excluded from the titration analysis. In addition, the presence of amine side groups in Amine SKL3 was expected to increase conductivity, potentially affecting the reliability of pH-meter readings. This chapter is organized into four main sections: Lignin, materials and chemicals, characterization of phenolic groups, FT-IR analysis, and quantification of antioxidant activity.

## 3.1 Lignin, materials, and chemicals

### 3.1.1 Lignin resources

Seven lignin types were investigated in this study. These include hardwood organosolv lignin (OSHL); softwood kraft lignin 1 (SKL1); softwood kraft lignin 2 (SKL2); and softwood kraft lignin 3 (SKL3). In addition, modified versions of OSHL, SKL1, and SKL3 were prepared according to the previously described procedure.[25], [26] These modified lignins include hydroxyethyl organosolv hardwood lignin (HEOSHL), hydroxyethyl softwood kraft lignin (HESKL1), and Aminated softwood kraft lignin (Amine SKL3). Table 3 summarizes the key information and corresponding sources for each lignin type.

**Table 3.** Overview of the key characteristics, relevant information, and corresponding sources of the different lignin types analyzed.

| Lignin | Wood category | Pulping method | Purification method | $M_n$ [KDa] | $M_w$ [KDa] | Description |
|---|---|---|---|---|---|---|
| OSHL | Hardwood | Organosolv | - | 2.07 [27] | 5.84 [27] | Suzano corporation, Brazil. |
| SKL1 | Softwood | Kraft | LignoBoost® | 1.15 [27] | 4.12 [27] | Domtar Corporation (USA) |
| SKL2 | Softwood | Kraft | Indulin AT | 1.2~1.34 [21] | 2.99~3.4 [21] | provided by Ingevity Corporation (South Carolina, USA) |
| SKL3 | Softwood | Kraft | LignoForce® | 6 [39] | 6~12.5[40] | donated by West Fraser (Alberta, Canada) |
| HEOSHL | Hardwood | Kraft | - | 2.72 [27] | 14.9 [27] | Liyang L., et al [27] |
| HESKL1 | Softwood | kraft | LignoBoost® | 0.92 [27] | 8.80 [27] | Liyang L., et al [27] |
| Amine SKL3 | Softwood | kraft | LignoForce® | 9.0 [25] | 43.3 [25] | Liyang L., et al [25] |

### 3.1.2 Chemicals

Sodium hydroxide pellets (NaOH, 40 g/mol), aqueous hydrochloric acid (HCl, 1 M), absolute ethanol (99.7 %), and dimethyl sulfoxide (DMSO, 99.7 %) were purchased from Sigma-Aldrich (Darmstadt, Germany). Deuterated chloroform ($CDCl_3$), anhydrous pyridine, chromium (III) 2,4-pentanedionate [$Cr(acac)_3$], *N*-hydroxy-5-norbornene-2,3-dicarboximide (NHND, 97%), ABTS(2,2′-Azino-bis(3-ethylbenzothiazoline-6-sulfonicacid)) diammonium salt, and potassium persulfate ($K_2S_2O_8$) were also from Sigma-Aldrich. DPPH (2,2-diphenyl-1-picrylhydrazyl) and Trolox (6-hydroxy-2,5,7,8-tetramethylchroman-2-carboxylic acid) were purchased from Sigma-Aldrich.

## 3.2 Phenol group characterization

Conductometric titration and Phosphorus-31 nuclear magnetic resonance spectroscopy ($^{31}P$ NMR) were performed to determine the number of phenol groups in lignin structure.

### 3.2.1 Conductometric titration analysis

Conductometric titration determines the number of phenol groups based on inflection points on the titration curve, obtained from constant conductivity measurements during the procedure.[25]

Oven-dried lignin (0.1 g) was dissolved in aqueous sodium hydroxide (0.1 M, 40 mL). The solution was titrated by adding HCl (0.1 M, ~60 mL) stepwise, under magnetic stirring, and at ambient temperature. Meanwhile, the conductivity of the solution was continuously recorded by a conductivity meter (CO301, VWR, Germany). (see Appendix C for experimental setup). The titrant volume was added to the lignin–NaOH solution following a flow rate schedule (mL/time). This addition rate was designed to enhance time efficiency and clearly identify the conductivity inflection points. Briefly, 5 mL of HCl was added every 5 minutes up to a total volume of 20 mL, followed by 1 mL per minute up to 25 mL, then 0.25 mL every 30 seconds up to 40 mL, and finally 1 mL every 30 seconds, corresponding to a total titrant volume of 60 mL.[25]

The titration curve was obtained by plotting conductivity (mS $cm^{-1}$) against titrant volume (mL) to visualize the inflection points. The derivative plot of the titration curve was generated, leading to the identification of four inflection points (A, B, C, D), illustrated in Figure 9 (a and b). The first inflection point, A, indicates the neutralization of the solution. Data points from A to B correspond to the volume interval in which the protonation of phenol groups occurs. The area between B and C corresponds to an

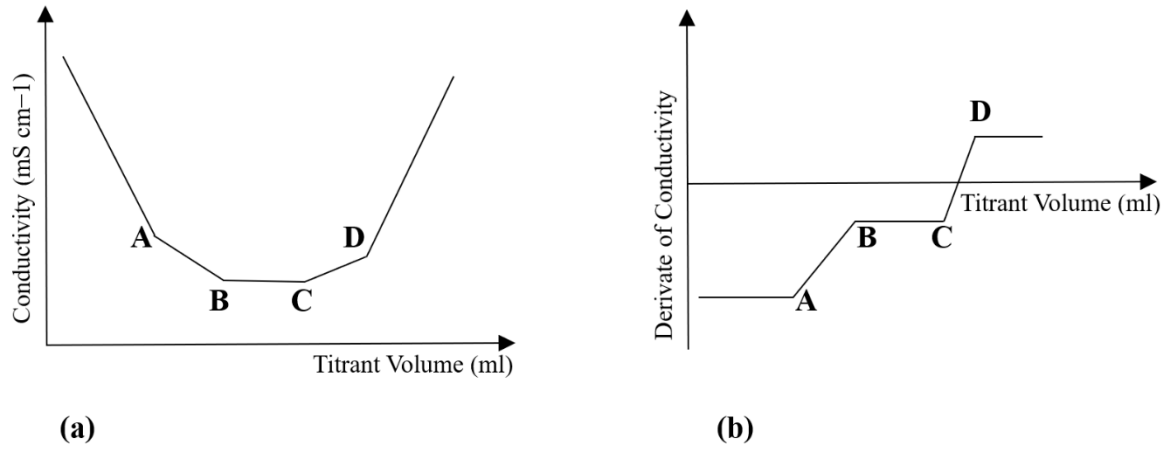


***Figure 9.*** *The picture of the titration curve (a) and its derivative (b).*

equilibrium state between protonation of phenol groups and carboxyl groups. Data points from C to D represent the protonation of carboxyl groups.

The calculation of the number of phenolic-OH groups in the lignin structure was performed using Equation 11. (See Appendix D for additional calculations used to derive Equation 11 and Appendix E for a detailed example calculation.)

$$\mathbf{N}[\boldsymbol{C_6H_5OH}] = \frac{(\boldsymbol{V_{B,HCl}} - \boldsymbol{V_{A,HCl}}) \times \boldsymbol{C_{HCl}}}{\boldsymbol{m_{lignin}}} \quad (11)$$

$N[C_6H_5OH]$ is the number of phenol groups, expressed in mmol per gram of lignin. $V_{B, HCl}$ is the total added HCl volume at point B, and $V_{A, HCl}$ is the total added HCl volume at point A. The HCl concentration ($C_{HCl}$) is equal to 0.1 M, and the lignin mass ($m_{Lignin}$) is 0.1 g.[25]

### 3.2.2 $^{31}$P NMR spectroscopy

The $^{31}$P NMR analysis was performed using a modified version of a protocol presented by Meng X et al.[11] Before analysis, three solutions were prepared; a solvent mixture (deuterated chloroform and anhydrous pyridine 1:1.6 (vol/vol)), a relaxation agent mixture (5.0 mg/mL solution of chromium (III) 2,4-pentanedionate (Cr(acac)3) in solvent mixture), and an internal standard (18.0 mg/mL of N-hydroxy-5-norbornene-2,3-dicarboximide (NDHD) in solvent mixture), which were prepared and stored in sealed containers.

Oven-dried lignin samples (20 mg) were mixed with 400µl of the solvent mixture, 100µl of internal standard, and 50µl of relaxation agent. The mixtures were vortexed carefully before adding 100 mL of the phosphorate agent (2-chloro-4,4,5,5-tetramethyl-1,3-2-dioxaphospholane (TMDP)) to the lignin solutions. The mixtures were vortexed thoroughly and transferred into a 5-mm NMR tube. The NMR tubes were placed in the measurement queue of the NMR spectrometer (600 MHz, Oxford magnet equipped with Bruker NEO console and 5mm QCIP 31P cold probe) at the Swedish NMR Centre in Gothenburg.[11]

The results were subsequently processed using TopSpin software (version 3.7.0, Bruker BioSpin GmbH).

The calculation of the phenolic -OH group was performed using Equation 12.

$$\frac{\boldsymbol{N[R-OH]}}{\boldsymbol{g\ of\ lignin}} = \frac{\boldsymbol{R \times mmol\ of\ NHND\ in\ NMR[mmol]}}{\boldsymbol{Dry\ weigth\ of\ lignin}} \quad (12)$$

Where $\frac{\mathrm{N[R-OH]}}{g\ of\ lignin}$ is the number of OH groups of the lignin's weight. R is the ratio of the integration of the spectral region of interest ($I_{OH}$) over the internal standard (IS) region ($I_{NHND}$), which is already calculated by the program, using Equation 13.

$$\boldsymbol{R = \frac{I_{OH}}{I_{NHND}} = \frac{Integration\ of\ spectral\ region\ of\ interest}{Intergration\ of\ NHND\ region}} \quad (13)$$

The mole quantity of the internal standard, which is mentioned as mmol of N-hydroxy-5-norbornene-2,3-dicarboximide (NHND-97%) in NMR in the equation above, is calculated using Equation 14:

$$\boldsymbol{mmol\ of\ NHND\ in\ NMR[mmol]} = \frac{\boldsymbol{m_{NHND}\ [g]}}{\boldsymbol{M_{NHND}\left[\frac{g}{mol}\right]}} \times \mathbf{97\%} \times \mathbf{1000} \qquad (14)$$

Where $m_{NHND}$ is the mass of NHND in grams, $M_{NHND}$ is the molecular weight of the NHND, which is 179.17 grams per mole.[11]

The utilized methods for phenol group characterization are compared in Table 4.

**Table 4.** An overview of the methodology characteristic of conductometric titration and $^{31}P$ NMR Spectroscopy

| Criteria | Conductometric titration | $^{31}P$ NMR spectroscopy |
|---|---|---|
| **Reagents** | Aqueousacids/bases (e.g., NaOH, HCl [11] | Derivatization reagents (e.g. TMDP), organic solvents. (e.g. Pyridine, $CDCl_3$)[11] |
| **Toxicity** | Low | High (organic solvents, phosphitylating agents) |
| **Ease of use** | Simple, accessible to most labs, can be performed by both manual and automatic | Complex, requires trained personnel and specialized equipment |
| **Equipments** | pH-meter, pipette, stirrer etc. (alternatively, auto titrator) | NMR spectrometer |
| **Calculation** | Basic stoichiometric calculations | Requires spectral integration, calibration, and TopSpin software.[11] |
| **Result consistency** | High reproducibility and reliability | Results can be affected due to the stability of the used reagents. |
| **Time consumption** | Quick (~36 minutes to 1 hour) | Time-consuming sample preparation and analysis (at least 24 hours inclusive queuing) |
| **Cost** | Cheap (Total price of the analysis~ 497 - 1680 SEK/sample[41]) | Expensive including instruments, time, reagents, maintenance, etc. ( Total price of the analysis ~528.00 US$[42]) |

## 3.3 FT-IR analysis

The Fourier Transform Infrared Spectroscopy (FT-IR) results were included and interpreted to obtain an overall view of lignin structure, by searching for other functional groups or structural characteristics that may promote antioxidant activity.

## 3.4 Antioxidant activity measurement

DPPH (2,2-diphenyl-1-picrylhydrazyl) radical scavenging activity and ABTS (2,2′-Azino-bis(3-ethylbenzothiazoline-6-sulfonicacid) radical scavenging activity are performed to measure the antioxidant activity in different types of lignin.

### 3.4.1 DPPH free radical scavenging capacity

DPPH analysis was performed using a modified version of the method described by Duan et al.[43] A DPPH stock solution (C = 0.6 mmol $L^{-1}$) was prepared with absolute ethanol. This solution was diluted (dilution factor = 1:10, C = 0.06 mmol $L^{-1}$) to achieve an absorbance below 1.000. Lignin samples were subsequently dissolved in DMSO (C = 0.05 mg $mL^{-1}$). Each lignin sample (0.13 mL) was mixed with 2.87 mL of diluted DPPH solution. A standard solution was prepared by mixing Trolox-DMSO solution (0.13 mL, C = 0.05 mg $mL^{-1}$) with 2.87 mL of diluted DPPH solution. Similarly, a control sample (2.87 mL DPPH solution and 0.13 mL DMSO) and a blank sample (2.87 mL pure ethanol and 0.13 mL DMSO) were prepared.

All mixtures were incubated in the dark for 30 minutes, and the DPPH concentrations were monitored over 300-700 nm using UV-Vis spectroscopy (SPECORD® PC 205, Analytik Jena, Germany). The absorbance at the peak maximum around 517 nm was used to calculate the radical scavenging activity of the samples using Equation 15. Measurements were performed in triplicate.

$$\boldsymbol{RSA_{DPPH}}[\%] = \left(\frac{\boldsymbol{ABS_{t=0} - ABS_{t=30\,min}}}{\boldsymbol{ABS_{t=0}}}\right) \times \mathbf{100} \tag{15}$$

Where, $RSA_{DPPH}$ stands for radical scavenging activity, and the $ABS_{t=30\ min}$, is the absorbance of the antioxidant + DPPH sample after 30 minutes of incubation. $ABS_{t=0}$ is the absorbance of the solution before any reaction occurred at time point 0, which consequently corresponds to the absorbance of the control sample.[29]

### 3.4.2 $ABTS^{+}$ radical scavenging assay

ABTS analysis was performed using a modified version of the method described by Rumpf et al.[29] An ABTS stock solution (10 mL, C = 7 mM) and a $K_2S_2O_8$ solution (10 mL, C = 2.25 mM) were prepared separately in distilled water. The solutions were mixed (1:1 v/v) and incubated in the dark for 16 hours at ambient temperature to generate the $ABTS^{\bullet+}$ radical cation solution. The $ABTS^{\bullet+}$ solution was diluted with distilled water at a 1:10 ratio to yield an absorbance of 0.700-1.000 at 734 nm. The appropriate $ABTS^{\bullet+}$ concentration was calculated using the Beer-Lambert law (see Appendix F for detailed calculations). The calculated concentration of $ABTS^{\bullet+}$ was 0.080 mM, which corresponds to an absorbance of 1.000 at 734 nm.

Lignin samples were dissolved in DMSO at a concentration of 0.5 mg $mL^{-1}$. Each sample solution (0.05 mL) was mixed with 2.5 mL of $ABTS^{\bullet+}$ solution. A control sample (0.05 mL DMSO and 2.5 mL $ABTS^{\bullet+}$ solution) and a blank sample (0.05 mL DMSO and 2.5 mL distilled water) were also prepared. The samples were incubated for 12 minutes, and the absorbance was measured against the blank over the wavelength range of 500–900 nm using UV-Vis spectroscopy (SPECORD® 205 PC, Analytik Jena, Germany). The absorbance at the peak maximum around 734 nm was used to calculate the radical scavenging activity (RSA) using Equation 17. All measurements were performed in triplicate.

$$\boldsymbol{RSA_{ABTS}} = \frac{\boldsymbol{A_{t=0} - A_{t=12min}}}{\boldsymbol{A_{t=0}}} \tag{17}$$

Where the $RSA_{ABTS}$ stands for radical scavenging activity of antioxidant toward ABTS, and the $A_{t=12min}$ is the absorbance of antioxidant + $ABTS^{+}$ sample after 12 minutes of incubation. $A_{t=0}$ is the absorbance of the solution before any reaction occurred at time point 0, which consequently corresponds to the absorbance of the control sample.[29]

# 4

# Results

The study results are presented in four key sections. Section 4.1 presents the quantification of the phenolic-OH group and lignin structure. Section 4.2 presents antioxidant activity measurement. Section 4.3 investigates any possible correlations between phenolic-OH group characterization and antioxidant activity. Lastly, Section 4.4 interprets the Fourier transform infrared (FT-IR) spectroscopy results.

## 4.1 Characterization of phenolic groups in lignin

This section presents the correlation analysis between different characterization methodologies for the phenolic -OH group. $^{31}$P NMR spectroscopy analysis was performed on all lignin types introduced in the methods section. For conductometric titration, however, the modified lignins were excluded from analysis. The reasons were incomplete dissolution of lignin in the solvent and the probable conductivity of the added amine group in Amine SKL3, which affected the pH-meter readings. Therefore, the correlation analysis between conductometric titration and $^{31}$P NMR spectroscopy was performed only on the original, unmodified lignin types, as presented in Figure 10.

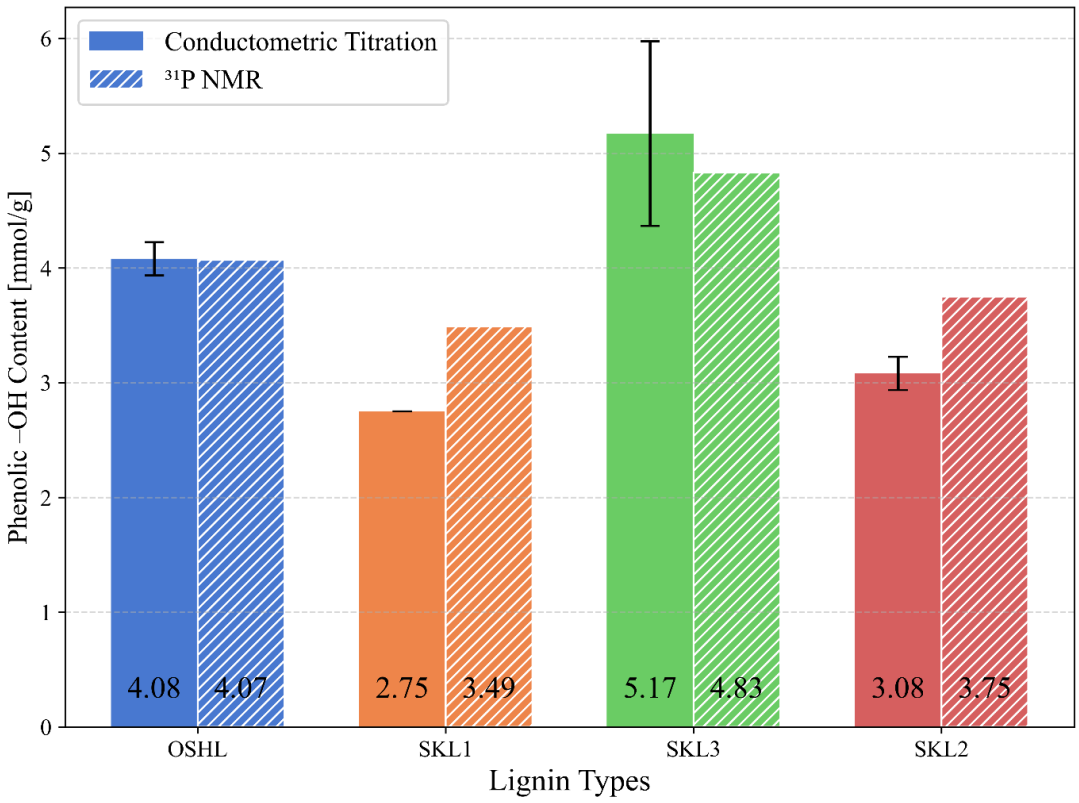


***Figure 10.*** *Results from phenol group characterization using conductometric titration and $^{31}$P NMR for OSHL, SKL1, SKL2, and SKL3 lignin. $^{31}$P NMR results are based on one sample per analysis. i.e., no error bars.*

### 4.1.1 Data analysis

The comparison in Figure 10 is performed on OSHL, SKL1, SKL2, and SKL3, showing that the reported phenolic-OH quantity for each lignin varies between two analyses, except for OSHL. This variation may be due to the different methods used to measure OH groups and the distinct reagents employed. At the same time, both analyses report the same sequence arrangement from lowest to highest number of phenolic -OH groups: SKL1 < SKL2 < OSHL < SKL3. The observed standard deviation in the conductometric titration analysis is small for all lignin types except SKL3, indicating the homogeneity and repeatability of the technique. Nevertheless, higher variability observed for SKL3 may be attributed to its lower solubility during the experimental procedure.

### 4.1.2 Linear regression analysis

A linear regression analysis was performed between the results from conductometric titration and $^{31}$P NMR, as presented in Figure 11.

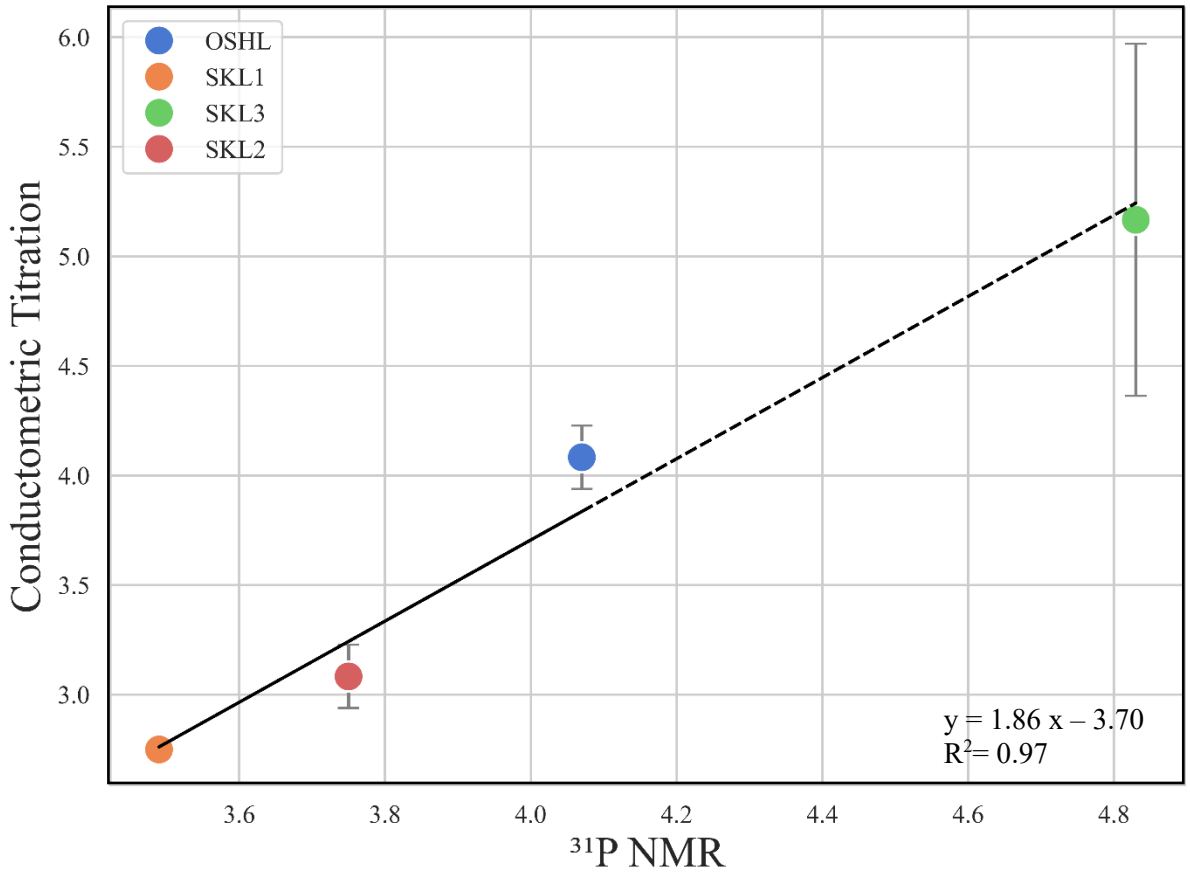


***Figure 11.*** *The linear regression analysis between the data obtained from conductometric titration, visualized on the x axis, and $^{31}$P NMR spectroscopy, visualized on the y axis.*

According to the analysis, a strong linear correlation was observed, with a slope of 1.85162 and an intercept of -3.70047. The obtained $R^2$ is equal to 0.97393, indicating that 97% of the variation in titration results can be explained by the corresponding $^{31}$P NMR values, meaning that results from both methodologies are linearly correlated.

### 4.1.3 Kendall's Tau, Spearman's, and Pearson's correlation analysis

The Spearman, Pearson, and Kendall's Tau correlation results are reported in Figure 12, reporting coefficients close to 1 in all analyses and indicating a strong positive correlation between the reported results from conductometric titration and $^{31}$P NMR.

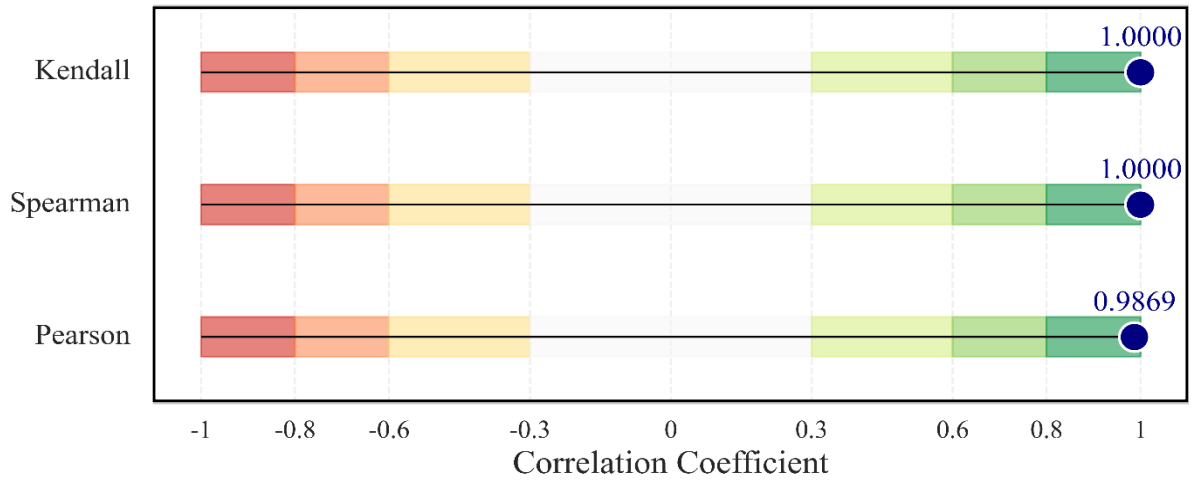


***Figure 12.*** *The Kendall's Tau, Spearman's, and Pearson's correlation coefficient between the data obtained from conductometric titration and $^{31}$P NMR spectroscopy.*

## 4.2 Antioxidant characterization of lignin

This section presents the results of antioxidant activity, determined by DPPH and ABTS radical scavenging analyses, and followed by a correlation analysis between these two methodologies. The investigation compared mean values from both assays and assessed their correlation using four methods: linear regression, Pearson's correlation, Spearman's correlation, and Kendall's Tau. Both radical scavenging assays were performed on seven lignin types: OSHL, SKL1, SKL2, SKL3, HESKL1, HEOSHL, and Amine SKL3.

### 4.2.1 Data analysis

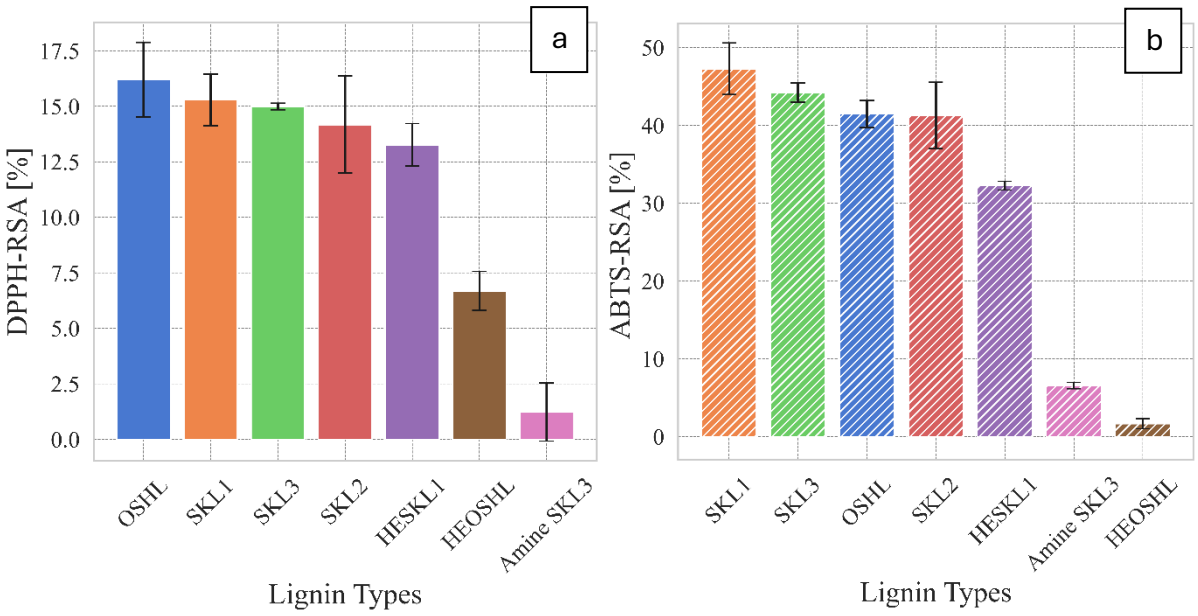


***Figure 13.*** *The radical scavenging activity (RSA) measured by DPPH (a) and ABTS (b) assays.*

Figure 13 presents a comparative summary of the DPPH and ABTS radical scavenging activities (RSA) for each lignin type.

According to Figure 13, the DPPH analysis suggested the following sequence of lignin from highest to lowest RSA_DPPH: OSHL>SKL1> SKL3> SKL2> HESKL1> HEOSHL >Amine SKL3. At the same time, ABTS analysis suggested the following sequence of lignin from highest to lowest RSA_ABTS: SKL1> SKL3> OSHL >SKL2>HESKL1> Amine SKL3> HEOSHL. In both analyses, the three least RSA belonged to the modified lignins: HEOSHL, HESKL1, and Amine SKL3. Among them, HESKL1 showed the best RSA. In contrast, the unmodified lignin types, OSHL, SKL1, SKL2, and SKL3, had the four highest RSA in both methodologies.

### 4.2.2 Linear regression analysis

A linear regression analysis was performed to evaluate the correlation between DPPH and ABTS analyses, presented in Figure 14.

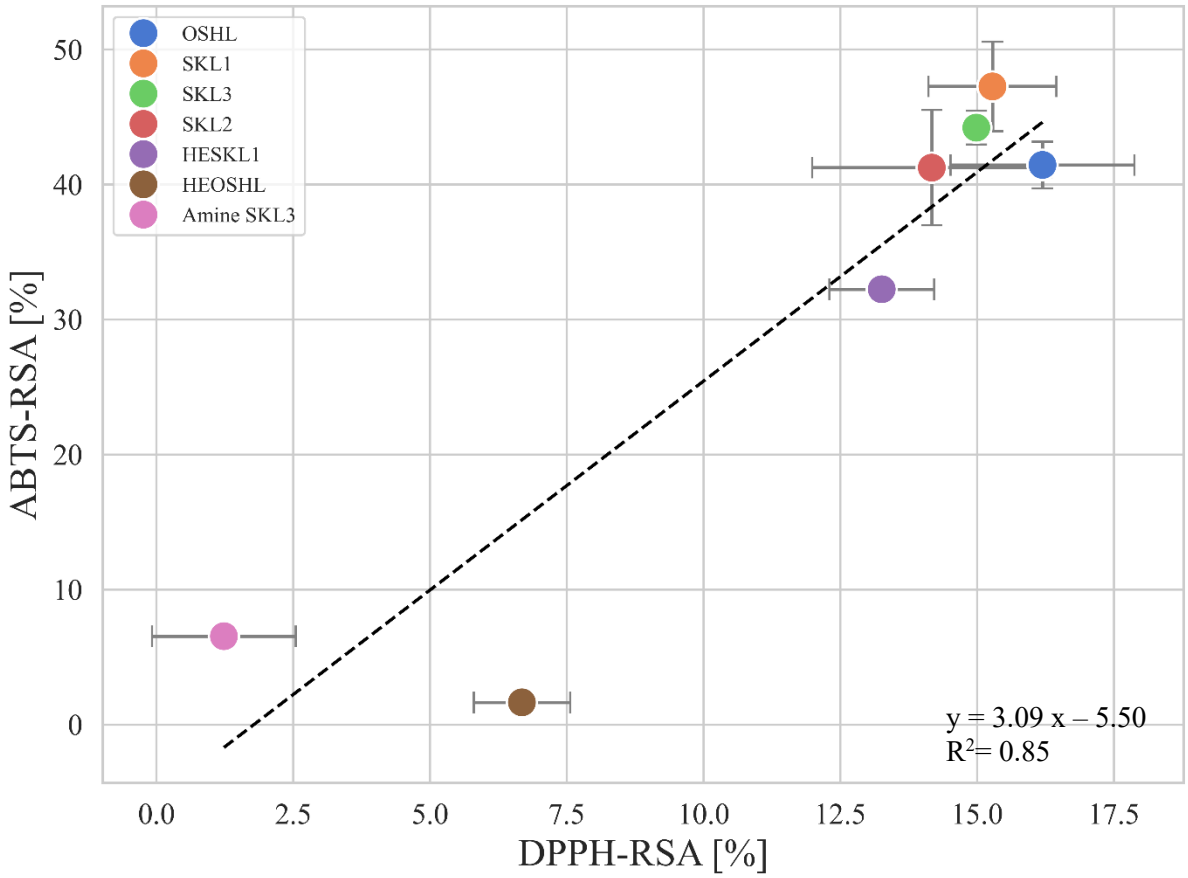


***Figure 14.*** *The linear regression analysis between the data obtained from DPPH radical scavenging activity, visualized on the x axis and ABTS radical scavenging activity, visualized on the y axis.*

The linear regression analysis generated a trendline with a slope of 3.09450, an intercept of -5.50416, and an $R^2$ value of 0.84814. This indicates that 85% of the variation in RSA_DPPH values can be explained by the corresponding RSA_ABTS values, demonstrating a strong linear correlation between the two methodologies.

### 4.2.3 Kendall's Tau, Spearman's, and Pearson's correlation analysis

Spearman, Pearson, and Kendall's Tau calculated coefficients were close to 1, as presented in Figure 15, demonstrating a strong positive correlation between the results of the DPPH and ABTS analyses.

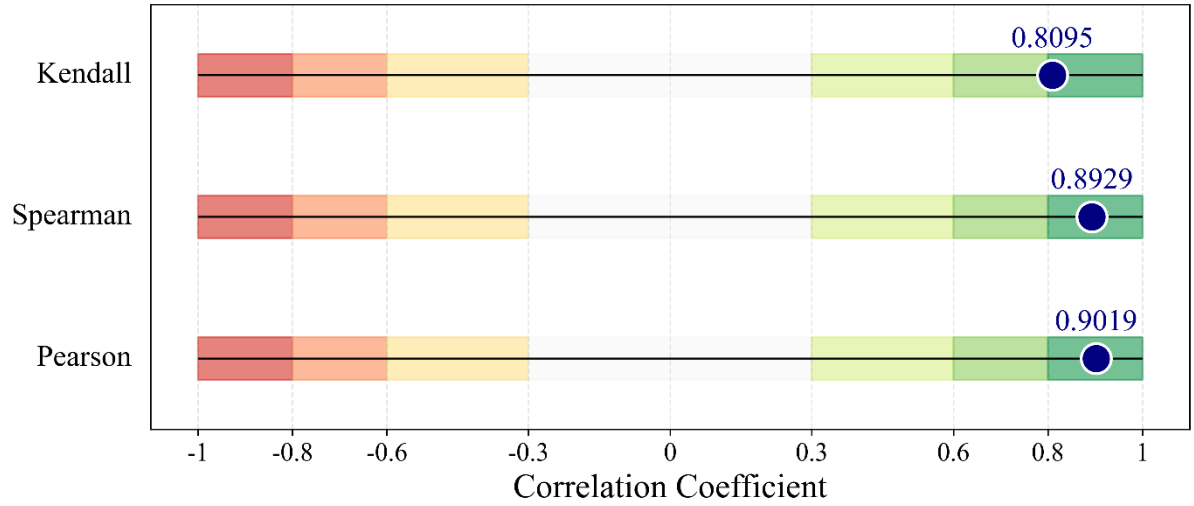


***Figure 15.*** *The Kendall's Tau, Spearman's, and Pearson's correlation coefficient between the data obtained from DPPH and ABTS analysis.*

## 4.3 Correlation analysis between phenol group quantity and antioxidant activity

This section introduces the correlation analysis results between phenolic-OH content and ABTS/DPPH-RSA, followed by linear regression, Pearson's, Spearman's, and Kendall's Tau analysis between RSA and $^{31}$P NMR, as presented in Section 4.3.1.

### 4.3.1 $^{31}$P NMR Vs radical scavenging activity

Figure 16 presents the linear correlation between $^{31}$P NMR results and radical scavenging activity.

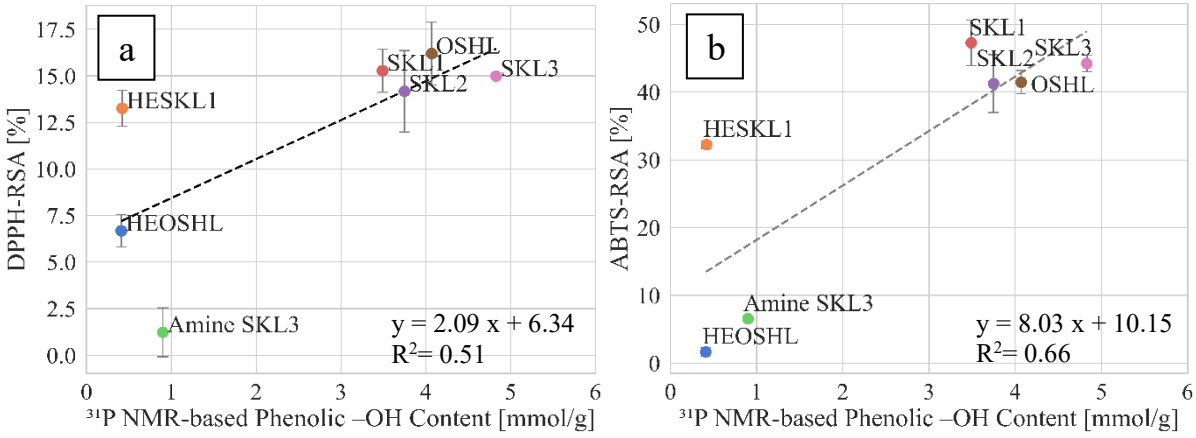


***Figure 16.*** *The linear regression correlation analysis between $^{31}$P NMR results and Radical scavenging activity: DPPH (a), and ABTS (b).*

The linear regression analysis presented in Figure 16a demonstrates a moderate linear correlation between $^{31}$P NMR-based phenolic-OH content and RSA_DPPH results. The regression equation has a slope of 2.09296 and an intercept of 6.34337. The $R^2$ value is 0.51, indicating that 51% of the variation in RSA_DPPH is explained by the obtained linear trend line with the $^{31}$P NMR-based phenolic-OH content.

According to the $^{31}$P NMR and ABTS correlation analysis (Figure 16b), the regression equation has a slope of 8.03317 and an intercept of 10.15183. The obtained $R^2$ is 0.66185, indicating that 66% of the variation in RSA_ABTS is explained by the obtained linear relationship with the $^{31}$P NMR-based phenolic content.

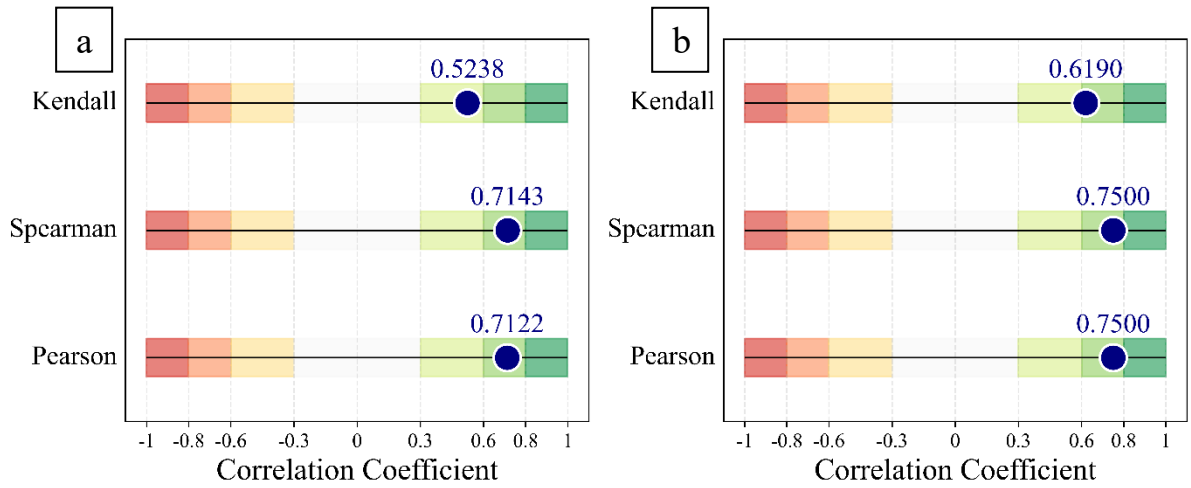


***Figure 17.*** *The Spearman's, Pearson's, and Kendall's Tau correlation coefficient between the data obtained from (a) $^{31}$P NMR spectroscopy and DPPH analysis, and (b) $^{31}$P NMR spectroscopy and ABTS analysis.*

Kendall's, Spearman's, and Pearson's correlation analyses are performed between the number of phenol groups obtained by $^{31}$P NMR, and the RSA-analyses obtained by DPPH and ABTS, presented in Figure 17. The results show a positive correlation across all three analyses, although the strength of the correlations is moderate.

## 4.4 Fourier Transform Infrared Spectroscopy (FT-IR) analysis

This section presents and interprets the results from Fourier Transform Infrared Spectroscopy (FT-IR) from a previous study by L. Liu et al[25]. Figure 18 introduces the result from the FI-TR analysis.

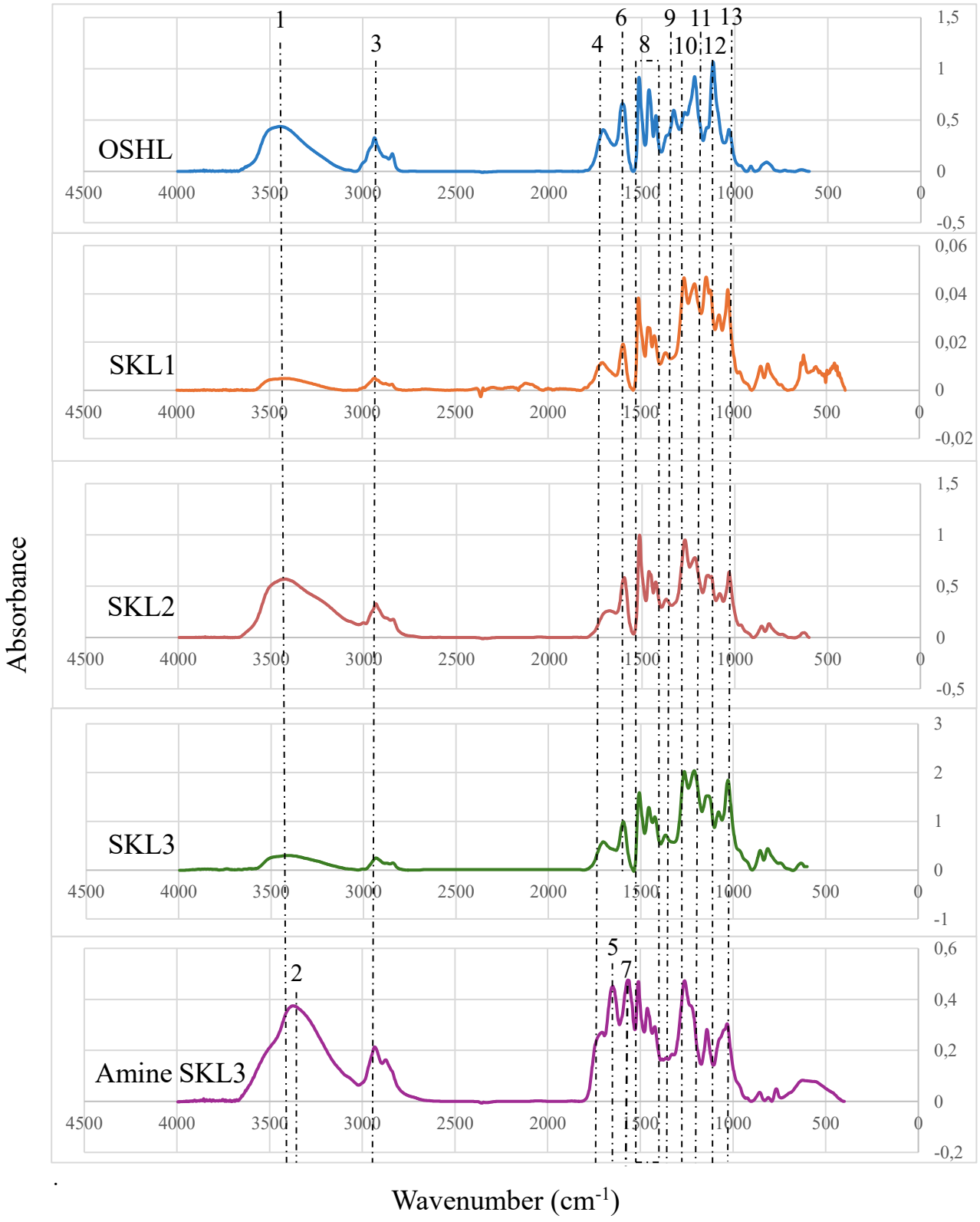


***Figure 18.*** *FT-IR spectra of OSHL, SKL1, SKL2, SKL3, and Amine SKL3.*

Chemical structures and functional groups identified in all five lignin types, along with their positions, are summarized in Table 5.
Among the observed positions, the wavelength interval [1685-1700] $cm^{-1}$ included several peaks for different types of lignin. The number and location of peaks in this specific area were unique for some lignin types. This region contains peaks corresponding to aromatics, conjugated groups, and carbonyl groups, which might be able to stabilize the phenolic radical formed after free-radical neutralization due to the resonance delocalization and stereoelectronic effects. These structures are primarily associated with lignin chromophores, such as quinones, stilbenes, catechols, aromatic ketones, and conjugated carbonyls with phenolics.[7] These findings suggest the hypothesis that these chromophores may also contribute to the antioxidant activity of lignin.

**Table 5**. Summarizes the identified chemical structures and functional groups in peak cluster 3 for OSHL, SKL1, SKL2, SKL3, and Amine SKL. The points are identified by *[25]* and the reference chart from Thermo Fisher.*[44]*

| **Peak** | **Peak position ($cm^{-1}$)** | **Description of the corresponding structure** |
|---|---|---|
| 1 | ~3445 | O-H stretching from alcohol/phenol group |
| 2 | ~3384 | N-H stretching from aliphatic primary amine |
| 3 | ~2937 | C-H stretching from alkane |
| 4 | ~1707 | carbonyl groups (C=O stretching from amid group or carboxylic acid or ester or aldehyde) |
| 5 | ~1651 | C=O stretching from urea/δ-lactam/conjugated ketone/ conjugated alkene |
| 6 | ~1597 | C-C stretching from lignin aromatic |
| 7 | ~1565 | N-H bending from amine |
| 8 | a) ~1514 | C-C stretching from the aromatic rings in lignin. |
| | b) ~1368 | |
| | c) ~1423 | |
| 9 | ~1371 | O-H bending from phenol |
| 10 | ~1270 | C-O stretching from alkyl-aryl ether and methoxy groups |
| 11 | ~1214 | C-O (H) + C-O (C) stretching from Aromatic OH +ether |
| 12 | ~1145 | C-N stretching from amine group or C-H bending from Guaiacyl unit |
| 13 | ~1031 | C-O (H) + C-O (C) stretching from Aliphatic OH + ether |

To obtain a qualitative measurement of the chromophore's peak in FT-IR analysis, a ratio between the height of peaks 4 and 8a is calculated for each lignin type. In this ratio, the height of peak 4 is a representative of carbonyl groups, while the height of peak 8a corresponds to the aromatic structures in lignin. A higher ratio between peak 4 and 8a indicates a higher chromophore content.

**Table 6.** Qualitative analysis of chromophore content in all lignin types by comparing the ration between peaks 4 and 8a.

| Lignin type | Peak 4 | Peak 8a | Ratio Peak (4/8a) | Ratio Percentage [%] | Ranking of chromophore content |
|---|---|---|---|---|---|
| **OSHL** | 0.40658 | 0.66002 | 0.616 | **62** | **1** |
| **SKL1** | 0.01132 | 0.0381 | 0.297 | **30** | **4** |
| **SKL2** | 0.26095 | 0.99457 | 0.262 | **26** | **5** |
| **SKL3** | 0.58226 | 1.58131 | 0.368 | **37** | **3** |
| **AMINE SKL3** | 0.27078 | 0.47046 | 0.575 | **58** | **2** |

The ratio analysis suggested that the chromophore content from highest to lowest is ranked as follows: OSHL >AMINE SKL3>SKL3> SKL1>SKL2. OSHL has significantly higher chromophore contents than SKL 1-3. All SKLs show similar chromophore contents (30 ± 7). Amine SKL3 also shows similar chromophore contents to OSHL.

# 5

# Discussion

This chapter is structured into four parts. Section 5.1 presents and discusses the results from the phenolic-OH group characterization, while Section 5.2 examines the results from the radical scavenging activity analysis. Section 5.3 explores the correlation between phenolic group characterization and radical scavenging activity. Finally, Section 5.4 introduces and discusses the results from the FT-IR analysis.

## 5.1 Conductometric titration analysis vs $^{31}$P NMR spectroscopy

Figure 10 displays the comparison of the conductometric titration and $^{31}$P NMR spectroscopy mean values of phenol groups. Although the methodologies report different OH values, both suggest the same ranking of lignin types: SKL1< SKL2< OSHL< SKL3 from lowest to highest phenolic-OH content. The standard deviation of conductometric titration analysis is also presented in Figure 10. The reported numbers are relatively small for OSHL and SKL2 and almost zero for SKL1, which indicates the results are reliable and reproducible. Several correlation analyses were performed to evaluate the degree of correlation between the two assays, illustrated in Figures 11 and 12.

The obtained $R^2$ is 0.97 for linear regression analysis. The reported values from Kendall's Tau, Spearman, and Pearson are 1 or very close to 1, indicating a perfect positive correlation between the number of phenolic hydroxyl groups obtained by titration and $^{31}$P NMR. These results show that, with optimizations, conductometric titration can replace $^{31}$P NMR spectroscopy as a simple, less toxic method for quantifying phenolic-OH groups.

### 5.1.1 Improvements

A limitation of these analyses was the small sample size. Titration analysis was performed in triplicate, and the mean values of the measurements are presented in Figure 10. $^{31}$P NMR spectroscopy was performed as a single replicate, leading to no reported standard deviation for the corresponding data. Conducting replicate measurements for the $^{31}$P NMR spectroscopy analysis represents an important area for methodological improvement.

The modified lignin types were excluded from the conductometric titration analysis due to conductivity and solubility challenges. Consequently, only four technical lignins were analyzed and compared for phenolic-OH characterization in this assay. This challenge limits the feasibility of robust statistical analyses due to insufficient sample size. It can be addressed by increasing the number of replicates and expanding the range of lignin types examined in future studies.

The modification of Amine SKL3 lignin involves the replacement of phenolic –OH groups with amine ($–NH_2$) groups, whereas in HEOSHL and HESKL1, the phenolic groups are substituted with aliphatic –OH groups. The amine and ester functionalities appear to interfere with conductivity measurements

during the titration analysis. A potential improvement to address this challenge would be to quantify the amine/ester group content and their respective conductivities on the modified lignin surfaces and incorporate these parameters into the calculation of phenolic content.

Another challenge encountered during the titration analysis was the limited solubility of certain lignins in the solvent system. Lignin is an amphiphilic macromolecule with complex structural characteristics, exhibiting variable solubility across different solvent systems. During the analysis, Amine SKL3 lignin did not fully dissolve in the aqueous sodium hydroxide solution, with a small fraction (<5%) remaining undissolved even after heating to approximately 50 °C (see Appendix G). Identifying a more suitable titrant solvent, applying elevated temperatures to enhance lignin dissolution, or incorporating an appropriate cosolvent to improve lignin solubility would be critical steps toward optimizing the titration protocol for future applications.

## 5.2 DPPH vs $ABTS^+$ radical scavenging assay

This section will review and discuss the results from radical scavenging activity, presented in Figures 13, 14, and 15.

The initial definition of antioxidant ability is to react with and neutralize free radicals. Consequently, radical scavenging activity (RSA) assays were chosen for a direct measurement of antioxidant activity. Due to the amphiphilic nature of lignin, both DPPH, which is suitable for hydrophobic components, and ABTS, which is suitable for both hydrophobic and hydrophilic components, are performed in this study. As shown in Figure 13, the ABTS and DPPH assays don't show identical rankings of antioxidant activity. At the same time, in both analyses, the three modified lignin types, Amine SKL3, HESKL1, and HEOSHL have relatively lower RSA. While the four original lignins, OSHL, SKL1, SKL2, and SKL3, have relatively higher RSA. This separation is significant. All modified lignin types have a fewer phenolic-OH groups. Both Amine SKL3 and HESKL1 are dephenolized derivatives of SKL3 and SKL1 and display lower antioxidant activity compared to their unmodified counterparts.

However, the reduction in antioxidant activity was less pronounced in HESKL1 than in Amine SKL3. Likewise, HEOSHL also showed a drastic decrease in antioxidant activity compared to its original version, OSHL. The results demonstrated that the phenolic content significantly influenced antioxidant activity, with SKL1 lignin exhibiting the highest RSA_ABTS and the second-highest RSA_DPPH, indicating very high antioxidant activity. This lignin type has the lowest phenol groups (Figure 10). Notably, even the dephenolized SKL1 lignin (HESKL1) still exhibited relatively high antioxidant activity. In other words, SKL1 exhibits high antioxidant activity, both with and without phenolic OH groups. Here, the phenolic-OH content does not seem to be the dominant factor in antioxidant activity. According to Figure 13, SKL3 has lower RSA than SKL1 in both analyses. Noteworthy that the SKL3 has the highest number of phenolic-OH than SKL1 (Figure 10). Here, the phenolic content doesn't seem to be the dominant factor influencing the antioxidant activity. However, this could be due to the lignin recovery process. SKL3 was isolated using the LignoForce® process, which includes an additional initial oxidation step compared to the LignoBoost® process used for SKL1; this extra oxidation step may slightly reduce antioxidant activity of SKL3. Lastly, SKL2 exhibited the lowest antioxidant activity among the original lignin types in both analyses.

To determine the strength of the linear correlation between DPPH and ABTS analysis, linear regression analysis is also performed and presented in Figure 14. Most of the original lignin types are clustered in the upper right of the scatter plot. Among these lignin types, SKL1 has significantly higher ABTS radical scavenging activity and is slightly separated from the rest of the cluster. OSHL, SKL1, SKL2, and SKL3 are clustered together. It is important to note that, although HESKL1 has a negligible number

of phenol groups compared to its original version SKL1, it has a slightly lower yet comparable RSA to unmodified lignin (Figure 13). This shows that, in addition to phenol groups, other structural features of HESKL1 result in a higher RSA than other modified lignins.

HEOSHL, the dephenolized version of OSHL, showed significantly lower RSA compared to its original form. This indicates that the exchange of phenolic-OH groups with aliphatic OH groups influences the antioxidant activity of this lignin type. Consequently, in addition to phenol groups, other structural features of HESKL1 result in higher RSA than those of other modified lignins. The modified Amine SKL3 exhibits the lowest antioxidant activity, as presented in both Figure 14 and Figure 15. As previously mentioned, in this modified lignin, most of the phenolic OH groups have been replaced by amine groups. According to the reported $^{31}P$ NMR results, approximately 74% of the phenolic content in Amine SKL is modified (×100 = 74.21%). This can be associated with the low RSA ability of this lignin type. According to Figure 14, the overall $R^2$ value showed a strong linear correlation between DPPH and ABTS analyses. ($R^2 = 0.85$) Kendall's tau, Spearman's, and Pearson's analyses demonstrated similar outcomes and showed that the results are reliable and reproducible. (see Figure 15)

In conclusion, the results obtained from Figures 13, 14, and 15 showed a strong correlation between the RSA results. Additionally, both Figures 13 and 14 demonstrate that modified lignin has lower RSA than the original lignin. HESKL1 is a noticeable exception to this; other structural features contributing to this increased RSA should be investigated in the future.

### 5.2.1 Improvements

The DPPH control was performed only once; consequently, no standard deviation or mean value is available for this data point. Although the control does not involve the reaction of interest and is only used to calculate RSA, performing the control in triplicate would improve consistency with the triplicate analysis conducted in other samples.

Furthermore, Amine SKL3 lignin exhibited limited solubility in DMSO, requiring an extended stirring time compared to other lignin types. The solution was continuously stirred for several days, whereas other lignin types achieved complete dissolution within 10 minutes. This difference in sample preparation represents a potential source of experimental variation. A negligible amount of Amine SKL3 lignin (< 1 mg) remained undissolved in DMSO, which may have influenced the observed antioxidant activity. Still, there is a significant difference in RSA between Amine SKL3 lignin and other lignin types, supported by two different protocols (see Figure 14). Therefore, this tiny solubility issue will not change the overall ranking of RSA.

A critical consideration in applying RSA_ABTS and RSA_DPPH methodologies is the optimization of the experimental protocol. Due to variations in lignin structure, material properties, and experimental conditions (including light exposure, temperature, and instrumentation), protocols reported in the literature may not yield optimal results. Factors such as stock solution concentration, lignin solution concentration, dilution factors, and the ratio between lignin and radical solutions must be optimized through preliminary experiments to ensure reliable results. It is essential to determine the appropriate solvent system specific to each lignin type under investigation. Furthermore, the absorbance of the control sample should be adjusted to fall within the absorbance range of 0.700–1.000 to ensure accurate measurements.

To address these challenges, multiple protocols were collected from the literature for both DPPH and ABTS analyses, and the methodologies were systematically evaluated and compared. Various solvents, concentrations, ratios, and dilution factors were tested during method development, ultimately leading to the establishment of optimized DPPH and ABTS protocols for this study.

## 5.3 Phenol group vs antioxidant activity

This section examines the correlation between phenolic groups and antioxidant activity, as analyzed in Figures 16 and 17.

Figure 16 presents linear regression analysis, correlating $^{31}$P NMR results with RSA values from DPPH and ABTS assays. The data show clear separation between modified lignins (HESKL1, HEOSHL, and Amine SKL3) and original lignins (OSHL, SKL1, SKL2, and SKL3), reflecting the lower phenolic-OH content in the modified samples. The $R^2$ values indicate moderate correlation between phenolic content (measured by $^{31}$P NMR) and RSA. Kendall's Tau, Spearman, and Pearson correlation analyses (Figures 17a and 17b) also support the linear regression results, confirming a weak positive correlation between phenolic-OH content and RSA activity for both DPPH and ABTS assays.

In summary, Figures 16 and 17 demonstrate a moderate correlation between phenolic -OH content and antioxidant activity when modified lignins are included in the analysis. However, among original lignins alone (Figure 16), no significant correlation exists between phenolic hydroxyl content and antioxidant activity. This supports the hypothesis that there are other factors determining lignin's antioxidant activity, requiring further investigation.

### 5.3.1 Improvement

The analysis has certain limitations, and there are areas for further improvement and refinement in future studies. Including a greater variety of lignin types and increasing the number of replicates can serve as valuable improvements in future studies.

Additionally, the only approach to antioxidant ability in this study was the measurement of radical scavenging activity using DPPH and ABTS. These protocols were chosen to evaluate the antioxidant capacity based on the definition of a material's antioxidant activity, which is the ability to react with and neutralize free radicals. However, considering the natural roles and characterizations in plant health, I hypothesize that lignin also has the capacity to avoid the creation of free radicals by absorbing environmental factors such as high temperatures, UV light, and antibacterial/antifungal agents. In other words, the role of lignin in providing health benefits is broader than the antioxidant activity of this natural component.

Although the mentioned point is not the focus of this study, further exploring the role of lignin in preventing free radical formation can be an important step toward its application as an antioxidant.

## 5.4 FT-IR analysis and identification of conjugated carbonyl groups

FT-IR analysis was used to investigate whether functional groups beyond phenolic -OH influence lignin's antioxidant activity. Such functional groups could stabilize themselves through reaction with free radicals, thereby contributing to antioxidant activity along with phenolic-OH groups.

The FT-IR spectra in Figure 18 show several common peaks across all lignin types. All samples exhibit O-H bond stretching of phenolic/alcoholic groups. However, Amine SKL lignin shows a specifically strong peak in this region due to amine groups substituting for phenolic groups. Aromatic ring peaks (three peaks at 1400-1520 $cm^{-1}$) also appear in all lignin types with minimal variation. Additionally, all samples contain C–O single bonds, corresponding to esters, alkyl-aryl ethers, and methoxy groups.

A particularly relevant region in the FT-IR analysis is the 1685-1700 $cm^{-1}$ interval. Investigated lignin types showed distinct peaks in this region. This area visualizes the peaks corresponding to the

conjugated and carbonyl groups stemming from various chemical structures. These Functional groups belong to chromophore structures such as quinones and stilbenes, which are responsible for color variation in lignin. They can also capture. They can also capture reactive electrons from free radicals, leading to radical scavenging activity. Ultimately, quantifying these functional groups could help explain the high antioxidant activity observed in lignins with lower phenolic content and is worthy of further investigation in future studies on lignin's antioxidant mechanisms.

Qualitative analysis of the chromophore content in lignin is presented in Table 6. The ranking of chromophore content showed a good correlation with the DPPH assay (Figure 13a). However, this did not correlate with the ABTS assay results (Figure 13b). Additionally, Amine SKL3 exhibited the second-highest chromophore content yet ranked among the weakest antioxidants in previous analyses (Figure 13a and b). The high chromophore ratio in this case could also be due to the amide groups in lignin.

In conclusion, chromophores (conjugated and carbonyl structures) emerged as potential contributors to lignin's antioxidant activity. However, the qualitative analysis did not show similar correlation trends between the chromophore quantity and the RSA assays.

### 5.4.1 Improvement

Future studies should identify more suitable methods for quantifying chromophores (e.g., NMR or UV) and investigate the of chromophore content on RSA.

Additionally, qualitative analysis was performed by calculating the ratio between the peak heights. A suggestion for improvement would be to apply the area under the peaks for the ratio calculation in future studies.

# 6

# Conclusions

This study investigated the correlation between phenolic-OH content and the antioxidant activity of lignin, while also examining other structural factors that may influence antioxidant properties. The key findings are as follows:

(1) Conductometric titration and $^{31}$P NMR spectroscopy showed a strong correlation ($R^2$ = 0.97), supported by Kendall's Tau, Spearman, and Pearson analyses (e.g., Kendall's coefficient = 1.00). These results demonstrate that conductometric titration is a promising method for determining phenolic content in unmodified lignins. It offers a less toxic, more environmentally friendly, and cost-effective alternative to $^{31}$P NMR spectroscopy. However, conductometric titration requires further refinement, particularly alternative solvents to improve lignin solubility, before it can be applied to diverse lignin types.

(2) Phenolic content moderately correlated with antioxidant activity ($R^2$ = 0.51 for $^{31}$P NMR vs. DPPH; $R^2$ = 0.66 for $^{31}$P NMR vs. ABTS), confirmed by Kendall's Tau, Spearman's, and Pearson's analyses (e.g., Kendall's coefficients: 0.51 and 0.66, respectively).

(3) This moderate correlation was inconsistent across samples. Notably, Hydroxyethyl softwood kraft lignin with no phenol group shows comparable antioxidant property to unmodified lignin with phenol -OH groups. These observations suggest that, along with phenolic OH, other characteristics in the lignin structure influence lignin's antioxidant activity (e.g., molar mass, dispersity, and chromophores).

(4) Chromophores may contribute to antioxidant activity through conjugation and carbonyl groups that stabilize free radicals. However, FT-IR qualitative analysis revealed no significant correlation between chromophore content and antioxidant activity. Further quantitative investigation combining FT-IR with complementary techniques (e.g., NMR) is needed to accurately quantify chromophore groups and clarify their role in antioxidant activity.

# References


[1] Neeraj Mandlekar, Aurélie Cayla, François Rault, Stéphane Giraud, Fabine Salaün, Giulio Malucelli, Jin-Ping Guan, 'An Overview on the Use of Lignin and Its Derivatives in Fire Retardant Polymer Systems', in *Lignin - Trends and Applications*, London: IntechOpen, 2018, p. 308. [Online]. Available: 10.5772/intechopen.68464

[2] D. S. Bajwa, G. Pourhashem, A. H. Ullah, and S. G. Bajwa, 'A concise review of current lignin production, applications, products and their environmental impact', *Industrial Crops and Products*, vol. 139, p. 111526, Nov. 2019, doi: 10.1016/j.indcrop.2019.111526.

[3] X. Lu, X. Gu, and Y. Shi, 'A review on lignin antioxidants: Their sources, isolations, antioxidant activities and various applications', *International Journal of Biological Macromolecules*, vol. 210, pp. 716–741, Jun. 2022, doi: 10.1016/j.ijbiomac.2022.04.228.

[4] S. L. Vavilala, S. B. Ghag, and J. S. D'Souza, 'Lignin: Understanding and Exploring Its Potential for Biofuel Production', in *Advanced Bioprocessing for Alternative Fuels, Biobased Chemicals, and Bioproducts*, Elsevier, 2019, pp. 165–186. doi: 10.1016/B978-0-12-817941-3.00009-7.

[5] P. S. Jiju, A. K. Patel, N. S. Shruthy, S. Shalu, C.-D. Dong, and R. R. Singhania, 'Sustainability through lignin valorization: recent innovations and applications driving industrial transformation', *Bioresour. Bioprocess.*, vol. 12, no. 1, p. 88, Aug. 2025, doi: 10.1186/s40643-025-00929-x.

[6] M. J. Suota *et al.*, 'Chemical and structural characterization of hardwood and softwood LignoForce™ lignins', *Industrial Crops and Products*, vol. 173, p. 114138, Dec. 2021, doi: 10.1016/j.indcrop.2021.114138.

[7] H. Zhang, S. Fu, and Y. Chen, 'Basic understanding of the color distinction of lignin and the proper selection of lignin in color-depended utilizations', *International Journal of Biological Macromolecules*, vol. 147, pp. 607–615, Mar. 2020, doi: 10.1016/j.ijbiomac.2020.01.105.

[8] K. Li, W. Zhong, P. Li, J. Ren, K. Jiang, and W. Wu, 'Recent advances in lignin antioxidant: Antioxidant mechanism, evaluation methods, influence factors and various applications', *International Journal of Biological Macromolecules*, vol. 251, p. 125992, Nov. 2023, doi: 10.1016/j.ijbiomac.2023.125992.

[9] E. Żymańczyk-Duda, B. Szmigiel-Merena, M. Brzezińska-Rodak, and M. Klimek-Ochab, 'Natural antioxidants–properties and possible applications', *JABB*, vol. 5, no. 4, Aug. 2018, doi: 10.15406/jabb.2018.05.00146.

[10] J. Lü, P. H. Lin, Q. Yao, and C. Chen, 'Chemical and molecular mechanisms of antioxidants: experimental approaches and model systems', *J Cellular Molecular Medi*, vol. 14, no. 4, pp. 840–860, Apr. 2010, doi: 10.1111/j.1582-4934.2009.00897.x.

[11] X. Meng *et al.*, 'Determination of hydroxyl groups in biorefinery resources via quantitative 31P NMR spectroscopy', *Nat Protoc*, vol. 14, no. 9, pp. 2627–2647, Sep. 2019, doi: 10.1038/s41596-019-0191-1.

[12] S. Sugiarto, Y. Leow, C. L. Tan, G. Wang, and D. Kai, 'How far is Lignin from being a biomedical material?', *Bioactive Materials*, vol. 8, pp. 71–94, Feb. 2022, doi: 10.1016/j.bioactmat.2021.06.023.

[13] M. Balk, P. Sofia, A. T. Neffe, and N. Tirelli, ‘Lignin, the Lignification Process, and Advanced, Lignin-Based Materials’, *IJMS*, vol. 24, no. 14, p. 11668, Jul. 2023, doi: 10.3390/ijms241411668.
[14] H. Sadeghifar and A. Ragauskas, ‘Lignin as a bioactive polymer and heavy metal absorber- an overview’, *Chemosphere*, vol. 309, p. 136564, Dec. 2022, doi: 10.1016/j.chemosphere.2022.136564.
[15] C. Crestini, H. Lange, M. Sette, and D. S. Argyropoulos, ‘On the structure of softwood kraft lignin’, *Green Chem.*, vol. 19, no. 17, pp. 4104–4121, 2017, doi: 10.1039/C7GC01812F.
[16] M. Bilal *et al.*, ‘Exploring the potential of ligninolytic armory for lignin valorization – A way forward for sustainable and cleaner production’, *Journal of Cleaner Production*, vol. 326, p. 129420, Dec. 2021, doi: 10.1016/j.jclepro.2021.129420.
[17] Q. Hua *et al.*, ‘Harnessing the synergistic power of lignin-Ecoflex blends for enhanced performance in food packaging’, *Chemical Engineering Journal*, vol. 499, p. 156139, Nov. 2024, doi: 10.1016/j.cej.2024.156139.
[18] X. Wan *et al.*, ‘Circular poly(ethylene terephthalate) with lignin-based toughening additives’, *Chemical Engineering Journal*, vol. 504, p. 158255, Jan. 2025, doi: 10.1016/j.cej.2024.158255.
[19] M. Garedew *et al.*, ‘Greener Routes to Biomass Waste Valorization: Lignin Transformation Through Electrocatalysis for Renewable Chemicals and Fuels Production’, *ChemSusChem*, vol. 13, no. 17, pp. 4214–4237, Sep. 2020, doi: 10.1002/cssc.202000987.
[20] C. Wu *et al.*, ‘Lignin decolorization in organic solvents and their application in natural sunscreen’, *International Journal of Biological Macromolecules*, vol. 237, p. 124081, May 2023, doi: 10.1016/j.ijbiomac.2023.124081.
[21] D. D. S. Argyropoulos *et al.*, ‘Kraft Lignin: A Valuable, Sustainable Resource, Opportunities and Challenges’, *ChemSusChem*, vol. 16, no. 23, p. e202300492, Dec. 2023, doi: 10.1002/cssc.202300492.
[22] P. Tomani *et al.*, ‘Integration of lignin removal into a kraft pulp mill and use of lignin as a bio-fuel’, *Cellulose Chemistry and Technology*, vol. 45, pp. 533–540, Sep. 2011.
[23] S. Bauer, H. Sorek, V. D. Mitchell, A. B. Ibáñez, and D. E. Wemmer, ‘Characterization of *Miscanthus giganteus* Lignin Isolated by Ethanol Organosolv Process under Reflux Condition’, *J. Agric. Food Chem.*, vol. 60, no. 33, pp. 8203–8212, Aug. 2012, doi: 10.1021/jf302409d.
[24] I. Haq, P. Mazumder, and A. S. Kalamdhad, ‘Recent advances in removal of lignin from paper industry wastewater and its industrial applications – A review’, *Bioresource Technology*, vol. 312, p. 123636, Sep. 2020, doi: 10.1016/j.biortech.2020.123636.
[25] L. Liu, X. Wan, S. Chen, P. Boonthamrongkit, M. Sipponen, and S. Renneckar, ‘Solventless Amination of Lignin and Natural Phenolics using 2-Oxazolidinone’, *ChemSusChem*, vol. 16, no. 15, p. e202300276, Aug. 2023, doi: 10.1002/cssc.202300276.
[26] L.-Y. Liu, K. Bessler, S. Chen, M. Cho, Q. Hua, and S. Renneckar, ‘In-situ real-time monitoring of hydroxyethyl modification in obtaining uniform lignin derivatives’, *European Polymer Journal*, vol. 142, p. 110082, Jan. 2021, doi: 10.1016/j.eurpolymj.2020.110082.

[27] L.-Y. Liu, Q. Hua, and S. Renneckar, 'A simple route to synthesize esterified lignin derivatives', *Green Chem.*, vol. 21, no. 13, pp. 3682–3692, 2019, doi: 10.1039/C9GC00844F.
[28] J. Li, X. Ran, M. Zhou, K. Wang, H. Wang, and Y. Wang, 'Oxidative stress and antioxidant mechanisms of obligate anaerobes involved in biological waste treatment processes: A review', *Science of The Total Environment*, vol. 838, p. 156454, Sep. 2022, doi: 10.1016/j.scitotenv.2022.156454.
[29] J. Rumpf, R. Burger, and M. Schulze, 'Statistical evaluation of DPPH, ABTS, FRAP, and Folin-Ciocalteu assays to assess the antioxidant capacity of lignins', *International Journal of Biological Macromolecules*, vol. 233, p. 123470, Apr. 2023, doi: 10.1016/j.ijbiomac.2023.123470.
[30] M. Azadfar, A. H. Gao, M. V. Bule, and S. Chen, 'Structural characterization of lignin: A potential source of antioxidants guaiacol and 4-vinylguaiacol', *International Journal of Biological Macromolecules*, vol. 75, pp. 58–66, Apr. 2015, doi: 10.1016/j.ijbiomac.2014.12.049.
[31] L. An, G. Wang, H. Jia, C. Liu, W. Sui, and C. Si, 'Fractionation of enzymatic hydrolysis lignin by sequential extraction for enhancing antioxidant performance', *International Journal of Biological Macromolecules*, vol. 99, pp. 674–681, Jun. 2017, doi: 10.1016/j.ijbiomac.2017.03.015.
[32] M. Shahzad Shirazi, M. Moridi Farimani, A. Foroumadi, K. Ghanemi, M. Benaglia, and P. Makvandi, 'Bioengineered synthesis of phytochemical-adorned green silver oxide (Ag2O) nanoparticles via Mentha pulegium and Ficus carica extracts with high antioxidant, antibacterial, and antifungal activities', *Sci Rep*, vol. 12, no. 1, p. 21509, Dec. 2022, doi: 10.1038/s41598-022-26021-4.
[33] J. F. Kadla and S. Kubo, 'Lignin-based polymer blends: analysis of intermolecular interactions in lignin–synthetic polymer blends', *Composites Part A: Applied Science and Manufacturing*, vol. 35, no. 3, pp. 395–400, Mar. 2004, doi: 10.1016/j.compositesa.2003.09.019.
[34] D. Kai *et al.*, 'Sustainable and Antioxidant Lignin–Polyester Copolymers and Nanofibers for Potential Healthcare Applications', *ACS Sustainable Chem. Eng.*, vol. 5, no. 7, pp. 6016–6025, Jul. 2017, doi: 10.1021/acssuschemeng.7b00850.
[35] H. A. Miot, 'Análise de correlação em estudos clínicos e experimentais', *J. vasc. bras.*, vol. 17, no. 4, pp. 275–279, Nov. 2018, doi: 10.1590/1677-5449.174118.
[36] D. D. Kiernan, *Natural Resources Biometrics*. Open SUNY Textbooks, 2014. [Online]. Available: https://milnepublishing.geneseo.edu/natural-resources-biometrics/
[37] K. Sarjana, E. Kurniawan, U. Lu'Luilmaknun, and N. M. I. Kertiyani, 'Analysis of Pre-Service Teacher's Performance Viewed by Creativity and Self-Regulated Learning', *j. kependidikan. has. penelit. kaji. kepustakaan. bid. pendidik. pengajaran. n.a.*, vol. 9, no. 1, p. 234, Mar. 2023, doi: 10.33394/jk.v9i1.6467.
[38] J. Liu, W. Tang, G. Chen, Y. Lu, C. Feng, and X. M. Tu, 'Correlation and agreement: overview and clarification of competing concepts and measures', vol. 28, no. 2, 2016.
[39] L.-Y. Liu, S. Chen, L. Ji, S.-K. Jang, and S. Renneckar, 'One-pot route to convert technical lignin into versatile lignin esters for tailored bioplastics and sustainable materials', *Green Chem.*, vol. 23, no. 12, pp. 4567–4579, 2021, doi: 10.1039/D1GC01033F.

[40] L. Kouisni, A. Gagné, K. Maki, P. Holt-Hindle, and M. Paleologou, 'LignoForce System for the Recovery of Lignin from Black Liquor: Feedstock Options, Odor Profile, and Product Characterization', *ACS Sustainable Chem. Eng.*, vol. 4, no. 10, pp. 5152–5159, Oct. 2016, doi: 10.1021/acssuschemeng.6b00907.
[41] Industridoktorn, 'Analyses and services', Industridoktorn, n.d. Accessed: Dec. 04, 2025. [Online]. Available: https://industridoktorn.se/en/analyses/
[42] Measurlabs, 'Lignin hydroxyl group content by 31P NMR spectroscopy', n.d. [Online]. Available: https://measurlabs.com/products/lignin-hydroxyl-group-content-by-31p-nmr-spectroscopy/
[43] X. Duan, X. Wang, J. Chen, G. Liu, and Y. Liu, 'Structural properties and antioxidation activities of lignins isolated from sequential two-step formosolv fractionation', *RSC Adv.*, vol. 12, no. 37, pp. 24242–24251, 2022, doi: 10.1039/D2RA02085H.
[44] Thermo Fisher, 'Organic functional group reference chart'. [Online]. Available: https://documents.thermofisher.com/TFS-Assets/CAD/posters/XX51346-E-0215M-OrganicFunctionalChart.pdf

# Appendices

## Appendix A. Code example for linear regression analysis between phenolic content obtained by $^{31}$P NMR, and RSA measurement obtained by DPPH analysis, performed in google colab.

```
import pandas as pd
import matplotlib.pyplot as plt
import seaborn as sns
import numpy as np
from scipy.stats import linregress
from matplotlib import font_manager as fm
from google.colab import files
# --- Introduce data ---
data = {
   'Lignin Types': ['OSHL', 'SKL1', 'SKL3', 'SKL2', 'HESKL1', 'HEOSHL', 'Amine SKL3'],
   'P31_NMR': ['4,07', '3,49', '4,83', '3,75', '0,42', '0,41', '0,9'],
   'DPPH-RSA': ['16,19595231', '15,28115372', '14,9861845', '14,17201873', '13,25744658', '6,679764333', '1,232186019'],
   'STD-DPPH': ['1,681853964', '1,167776993', '0,146906465', '2,185404652', '0,957568638', '0,879459354','1,31380854982016'],
}
# --- Create DataFrame ---
df = pd.DataFrame(data)
# --- Convert strings with commas to floats ---
for col in ['P31_NMR', 'DPPH-RSA', 'STD-DPPH']:
   df[col] = df[col].str.replace(',', '.').astype(float)
# --- Sort DataFrame by P31_NMR ---
df_sorted = df.sort_values(by='P31_NMR')
# --- Scatter plot with error bars ---
plt.figure(figsize=(8, 6), dpi=1000)  # Large figure
sns.set(style="whitegrid")
# Get muted color palette
muted_palette = sns.color_palette("muted", len(df_sorted))
# Plot points with error bars
for i, color in enumerate(muted_palette):
   plt.errorbar(
      df_sorted['P31_NMR'].iloc[i],
      df_sorted['DPPH-RSA'].iloc[i],
      yerr=df_sorted['STD-DPPH'].iloc[i],
      fmt='o',
      color=color,
      capsize=5,
      ecolor='gray',
      markersize=10
   )
   plt.text(
      df_sorted['P31_NMR'].iloc[i] + 0.05,
      df_sorted['DPPH-RSA'].iloc[i],
      df_sorted['Lignin Types'].iloc[i],
      fontsize=23,
      weight='bold',
      fontproperties=font_prop
   )
# --- Linear regression analysis ---
slope, intercept, r_value, p_value, std_err = linregress(df_sorted['P31_NMR'], df_sorted['DPPH-RSA'])
r_squared = r_value ** 2

# Plot regression line
x_vals = np.linspace(df_sorted['P31_NMR'].min(), df_sorted['P31_NMR'].max(), 100)
y_vals = slope * x_vals + intercept
plt.plot(x_vals, y_vals, color='black', linestyle='--', linewidth=2)
# --- Labels and styling ---
plt.xlabel('³¹P NMR-based Phenolic –OH Content [mmol/g]', fontproperties=font_prop, fontsize=24)
plt.ylabel('DPPH-RSA [%]', fontproperties=font_prop, fontsize=24)
plt.xticks(fontproperties=font_prop, fontsize=22)
```

```
plt.yticks(fontproperties=font_prop, fontsize=22)
plt.xlim(0, 6)
plt.tight_layout()
# --- Save figure high-quality ---
plt.savefig('DPPH_OH.png', dpi=1000, bbox_inches='tight', facecolor='white')
plt.savefig('DPPH_OH.pdf', bbox_inches='tight', facecolor='white')
# --- Show plot ---
plt.show()
# --- Download files ---
files.download('DPPH_OH.png')
files.download('DPPH_OH.pdf')
# --- Print regression stats with 4 decimals ---
print(f"Slope: {slope:.4f}")
print(f"Intercept: {intercept:.4f}")
print(f"R²: {r_squared:.4f}")
print(f"P-value: {p_value:.4f}")
print(f"Standard Error: {std_err:.4f}")
```

**Appendix B. Calculation example for Kendall Tau analysis. Example Calculation for DPPH-RSA and N[-OH]**

The first step in this analysis is to sort the lignin types from the highest to lowest based on one factor, phenolic content (N[-OH]) in this case. Later, the corresponding antioxidant activity measurement (AO-properties) will be written in front of each lignin type. Both factors will be ranked from highest to lowest in the next two columns. (N[-OH]-RANK and AO-RANK)

**Table 7.** The phenolic -OH content (N[-OH]), and the antioxidant activity (RSA) and their ranking.

| Lignin Types | Sorted Lignin Types | N[-OH] | RSA | N[-OH]-RANK | AO-RANK |
|---|---|---|---|---|---|
| OSHL | SKL3 | 4.998333 | 29.59733541 | 1 | 2 |
| SKL1 | OSHL | 4.076667 | 28.82299135 | 2 | 3 |
| SKL3 | SKL2 | 3.416667 | 27.71010598 | 3 | 4 |
| SKL2 | SKL1 | 3.12 | 31.27213673 | 4 | 1 |
| HESKL1 | Amine SKL3 | 0.9 | 3.891243063 | 5 | 7 |
| HEOSHL | HESKL1 | 0.42 | 22.75052696 | 6 | 5 |
| Amine SKL3 | HEOSHL | 0.41 | 4.165797966 | 7 | 6 |

Based on the obtained ranks for the other factor (AO- RANK in this case), the number of concordant and discordant will be calculated by considering each rank from the top to bottom and comparing it to all ranks below it. If the rank is higher, it is a concordant (= 1), and if the rank is lower it is a discordant (= 0). For example, the first cell in the AO-RANK column (the purple cell), is equal to 2. The cell below the purple cell has a higher rank (the green cell), and is therefore a concordant and equal to 1, which is placed in front of the same rank in the third column (the yellow cell). The procedure will continue throughout the whole column and for each rank separately. As seen in table below, the columns A to F correspond to the analysis of ranks A to F. The number of ones results in the number concordants, while the number of zeros correspond to the number of discordants.

| | N[-OH]-RANK | AO-RANK | A | B | C | D | E | F |
|---|---|---|---|---|---|---|---|---|
| A | 1 | 2 | | | | | | |
| B | 2 | 3 | 1 | | | | | |
| C | 3 | 4 | 1 | 1 | | | | |
| D | 4 | 1 | 0 | 0 | 0 | | | |
| E | 5 | 7 | 1 | 1 | 1 | 1 | | |
| F | 6 | 5 | 1 | 1 | 1 | 1 | 0 | |
| G | 7 | 6 | 1 | 1 | 1 | 1 | 0 | 1 |
| The number of concordant pairs ($n_c$) | | | | | | | 16 | |
| The number of discordant pairs($n_d$) | | | | | | | 5 | |
| The total number of pairs($n_t$) | | | | | | | 21 | |

$$n_t = \frac{1}{2}n(n-1) = n_c + n_d = 21$$

$$\hat{\tau} = \frac{n_c - n_d}{n_t} = \frac{16-5}{21} = 0.52$$

$\hat{\tau}$ varies between -1 and 1, with -1 corresponding to the perfect discordance, 0 indicating no association between the variables, and 1 corresponding to the perfect concordance. $\hat{\tau} = 0.52$ corresponds to a moderately positive correlation between RSA_DPPH and N[-OH].

## Appendix C. Conductometric titration experiment setup

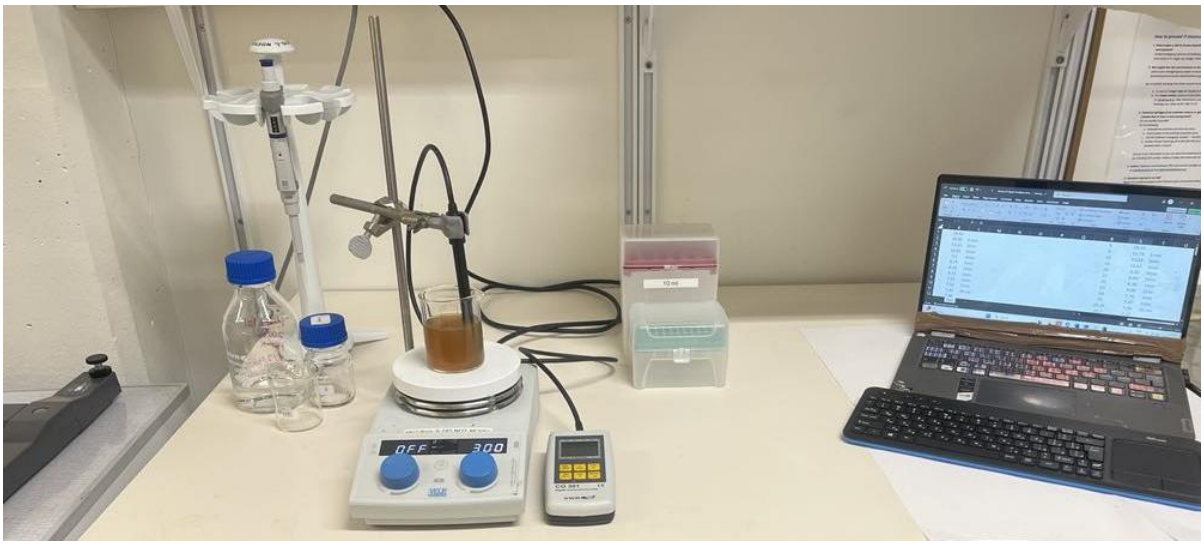

***Figure 19**. Experiment set up for conductometric titration*

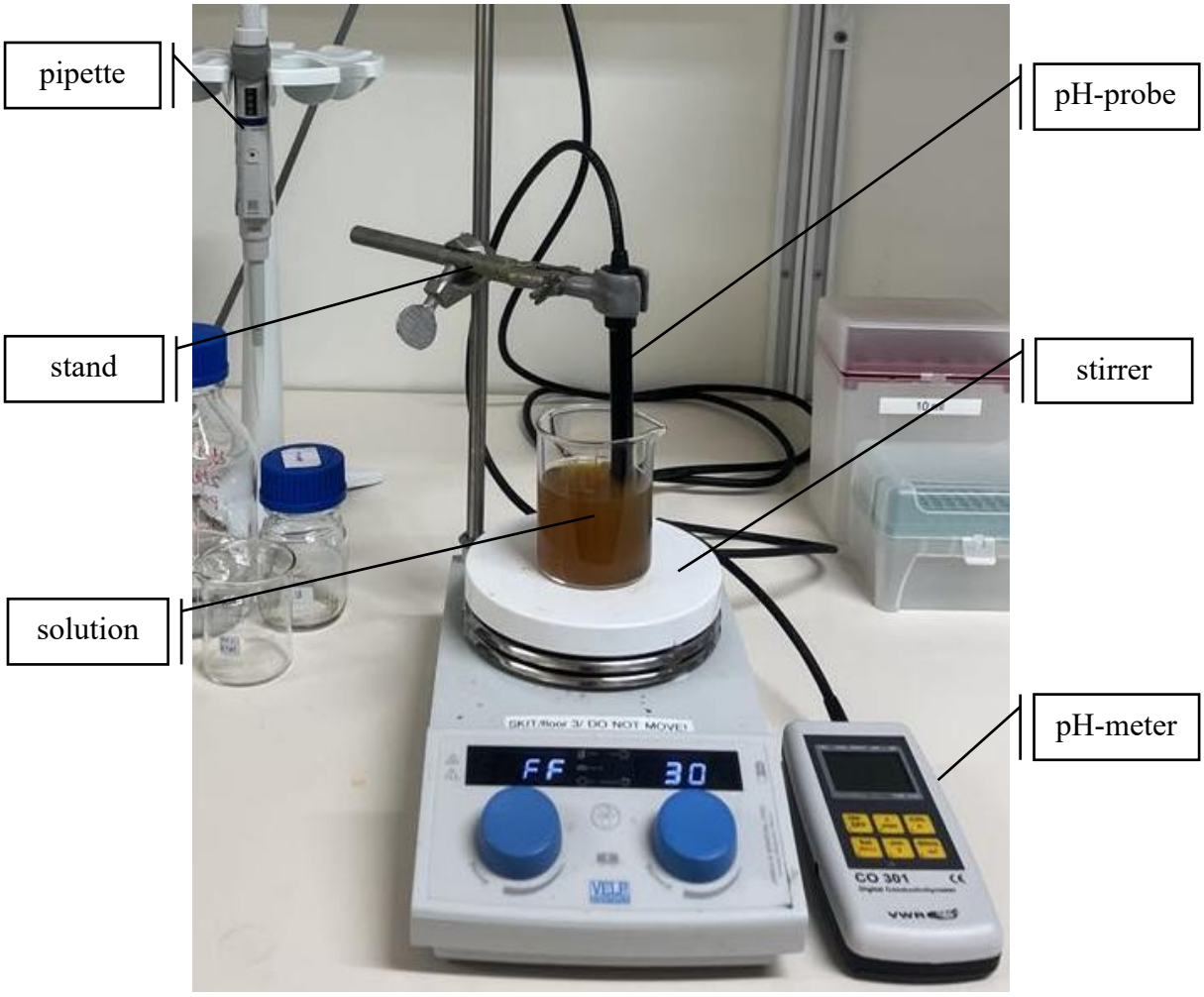


***Figure 20.** Implied instruments in the experiment set up for conductometric titration.*

**Appendix D. Description for the formula to calculate lignin's phenolic hydroxyl group content [mol/g]**

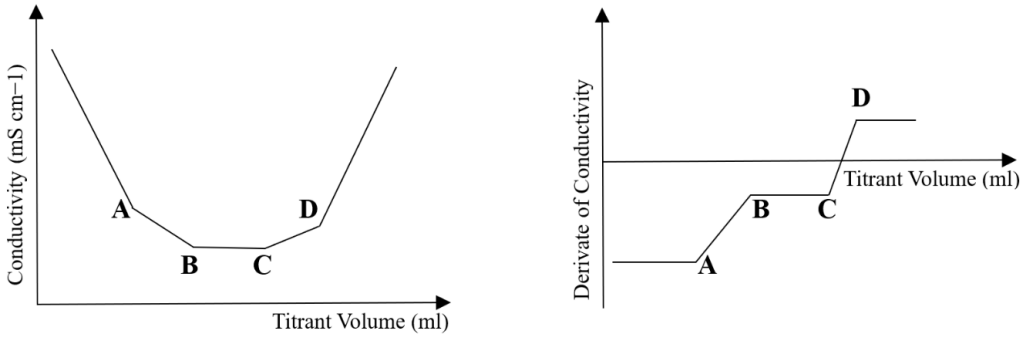


**(a)** **(b)**

***Figure 21.*** *The picture of the titration curve (a) and its derivative (b).*

Between points A and B, the titrant HCl is reacting with the phenolic hydroxyl groups. The reaction is as follows:

$$\boldsymbol{C_6H_5OH + HCl \rightarrow C_6H_5OCl + H_2O}$$

In this reaction 1 mol of the phenol groups reacts with 1 mol of HCl.

$$\boldsymbol{n[C_6H_5OH] = n[HCl]}$$

Where the $\boldsymbol{n[C_6H_5OH]}$ is the amount of phenolic -OH and $\boldsymbol{n[HCl]}$ is the amount of HCl in moles. Therefore, the number of phenol groups on the lignin surface can be calculated based on the added HCl between points A and B, which is equal to the amount of HCl that reacts with the phenolic hydroxyl groups using the formula below.

$$\boldsymbol{C}\left[\frac{mol}{cm^3}\right] = \frac{\boldsymbol{n}[mol]}{\boldsymbol{V}[cm^3]} \quad \rightarrow \quad \boldsymbol{n[mol] = C}\left[\frac{mol}{cm^3}\right] \times \boldsymbol{V}[cm^3]$$

$$\boldsymbol{n[C_6H_5OH] = C[C_6H_5OH] \times V[C_6H_5OH]}$$

$$\boldsymbol{n[C_6H_5OH] = n[HCl]}$$

$$\boldsymbol{n[C_6H_5OH] = C[HCl] \times V[HCl]}$$

Where C is the concentration of HCl, and V is the volume of added HCl. Lastly, the amount of phenolic-OH can be calculated using the amount of HCl added to the solution through the following formula.

$$\boldsymbol{N[C_6H_5OH] = C[HCl] \times V[HCl]_{AB}}$$

$$\boldsymbol{NV[HCl]_{AB} = V_{B,HCL} - V_{A,HCL}}$$

$$\boldsymbol{N}\left[\frac{mol}{g}\right] = \frac{\boldsymbol{n}[mol]}{\boldsymbol{m}[g]\ lignin}$$

$$\mathbf{N}[\boldsymbol{C_6H_5OH}] = \frac{(\boldsymbol{V_{B,HCL} - V_{A,HCL}}) \times \boldsymbol{C_{HCL}}}{\boldsymbol{m_{lignin}}}$$

In the obtained formula, $N[C_6H_5OH]$ is the number of phenol groups, expressed in mmol per gram of lignin. $V_{B, HCl}$ is the total added HCl volume at point B, and $V_{A, HCl}$ is the total added HCl volume at point A. The HCl concentration ($C_{HCl}$) is equal to 0.1 M. and the lignin mass ($m_{Lignin}$) is 0.1 g, due to the experiment instructions.

## Appendix E. Example of timing schedule, titration curve, titration curve's derivative, and calculation of phenolic hydroxyl groups number $\mathbf{N}[C_6H_5\mathbf{OH}]$ for SKL2.

**Table 8.** Data from conductometric titration analysis of SKL2.

| Volume[ml] | Conductivity[mS] | d(cond.)/d(vol.) | waiting time |
|---|---|---|---|
| 0 | 19,18 | -0,702 | |
| 5 | 15,67 | -0,554 | 5 min |
| 10 | 12,9 | -0,438 | 3min |
| 15 | 10,71 | -0,366 | 3min |
| 20 | 8,88 | -0,34 | 3min |
| 21 | 8,54 | -0,32 | 1min |
| 22 | 8,22 | -0,31 | 1min |
| 23 | 7,91 | -0,3 | 1min |
| 24 | 7,61 | -0,28 | 1min |
| 25 | 7,33 | -0,28 | 1min |
| 25,25 | 7,26 | -0,28 | 30sec |
| 25,5 | 7,19 | -0,32 | 30sec |
| 25,75 | 7,11 | -0,28 | 30sec |
| 26 | 7,04 | -0,28 | 30sec |
| 26,25 | 6,97 | -0,28 | 30sec |
| 26,5 | 6,9 | -0,24 | 30sec |
| 26,75 | 6,84 | -0,28 | 30sec |
| 27 | 6,77 | -0,24 | 30sec |
| 27,25 | 6,71 | -0,28 | 30sec |
| 27,5 | 6,64 | -0,28 | 30sec |
| 27,75 | 6,57 | -0,24 | 30sec |
| 28 | 6,51 | -0,24 | 30sec |
| 28,25 | 6,45 | -0,24 | 30sec |
| 28,5 | 6,39 | -0,24 | 30sec |
| 28,75 | 6,33 | -0,2 | 30sec |
| 29 | 6,28 | -0,24 | 30sec |
| 29,25 | 6,22 | -0,24 | 30sec |
| 29,5 | 6,16 | -0,2 | 30sec |
| 29,75 | 6,11 | -0,2 | 30sec |
| 30 | 6,06 | -0,2 | 30sec |
| 30,25 | 6,01 | -0,2 | 30sec |
| 30,5 | 5,96 | -0,16 | 30sec |
| 30,75 | 5,92 | -0,2 | 30sec |
| 31 | 5,87 | -0,12 | 30sec |
| 31,25 | 5,84 | -0,12 | 30sec |
| 31,5 | 5,81 | -0,12 | 30sec |
| 31,75 | 5,78 | -0,12 | 30sec |
| 32 | 5,75 | -0,08 | 30sec |
| 32,25 | 5,73 | -0,08 | 30sec |
| 32,5 | 5,71 | -0,08 | 30sec |
| 32,75 | 5,69 | -0,04 | 30sec |
| 33 | 5,68 | -0,08 | 30sec |
| 33,25 | 5,66 | -0,04 | 30sec |
| 33,5 | 5,65 | -0,08 | 30sec |
| 33,75 | 5,63 | -0,04 | 30sec |
| 34 | 5,62 | -0,04 | 30sec |
| 34,25 | 5,61 | -0,04 | 30sec |
| 34,5 | 5,6 | -0,04 | 30sec |
| 34,75 | 5,59 | -0,04 | 30sec |
| 35 | 5,58 | -0,04 | 30sec |
| 35,25 | 5,57 | 0 | 30sec |
| 35,5 | 5,57 | 0 | 30sec |
| 35,75 | 5,57 | 0 | 30sec |
| 36 | 5,57 | -0,08 | 30sec |
| 36,25 | 5,55 | 0 | 30sec |
| 36,5 | 5,55 | -0,04 | 30sec |
| 36,75 | 5,54 | -0,04 | 30sec |
| 37 | 5,53 | -0,04 | 30sec |
| 37,25 | 5,52 | 0 | 30sec |
| 37,5 | 5,52 | 0 | 30sec |
| 37,75 | 5,52 | -0,04 | 30sec |
| 38 | 5,51 | -0,04 | 30sec |
| 38,25 | 5,5 | 0,04 | 30sec |
| 38,5 | 5,51 | 0,08 | 30sec |
| 38,75 | 5,53 | 0,24 | 30sec |
| 39 | 5,59 | 0,28 | 30sec |
| 39,25 | 5,66 | 0,36 | 30sec |
| 39,5 | 5,75 | 0,36 | 30sec |
| 39,75 | 5,84 | 0,36 | 30sec |
| 40 | 5,93 | 0,39 | 30sec |
| 41 | 6,32 | 0,38 | 30sec |
| 42 | 6,7 | 0,37 | 30sec |
| 43 | 7,07 | 0,37 | 30sec |
| 44 | 7,44 | 0,35 | 30sec |
| 45 | 7,79 | 0,36 | 30sec |
| 46 | 8,15 | 0,33 | 30sec |
| 47 | 8,48 | 0,33 | 30sec |
| 48 | 8,81 | 0,32 | 30sec |
| 49 | 9,13 | 0,32 | 30sec |
| 50 | 9,45 | 0,31 | 30sec |
| 51 | 9,76 | 0,3 | 30sec |
| 52 | 10,06 | 0,31 | 30sec |
| 53 | 10,37 | 0,3 | 30sec |
| 54 | 10,67 | 0,29 | 30sec |
| 55 | 10,96 | 0,29 | 30sec |
| 56 | 11,25 | 0,27 | 30sec |
| 57 | 11,52 | 0,27 | 30sec |
| 58 | 11,79 | 0,27 | 30sec |
| 59 | 12,06 | 0,26 | 30sec |
| 60 | 12,32 | 0,205333333 | 30sec |

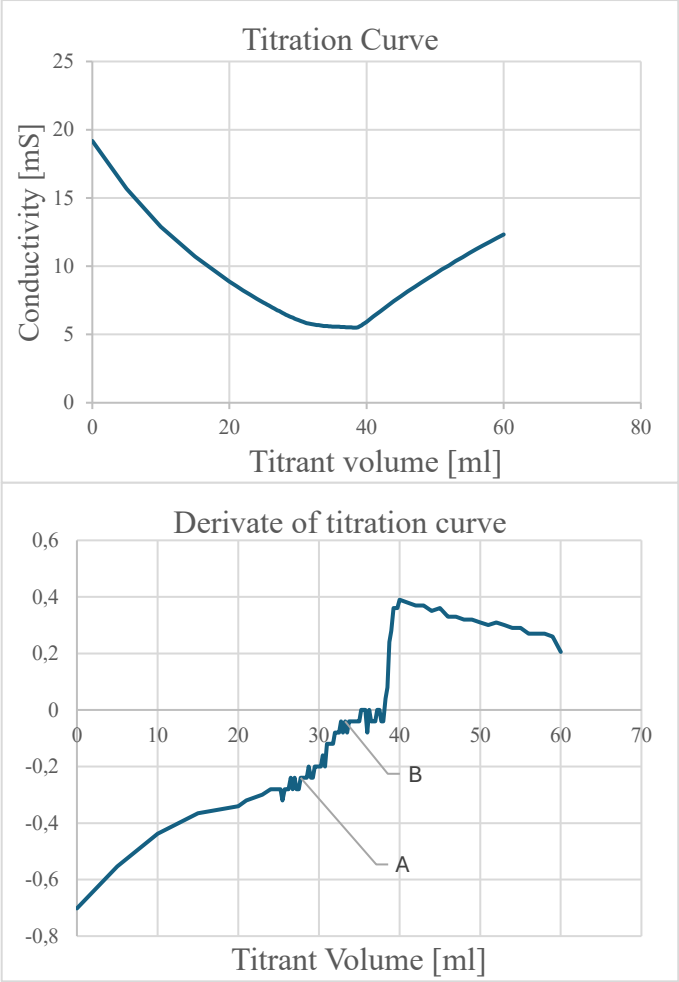


***Figure 22.*** *The example titration curve (a) and the derivate of the titration curve (b)*

**Table 9.** Determined points of Phenolic -OH group's reacting interval (A and B), and carboxyl group's reaction area (C and D)

| Points | Volumes |
|---|---|
| A | 30.75 |
| B | 33.75 |
| C | 38.5 |
| D | 40 |

$$\mathbf{N}[C_6H_5\mathbf{OH}] = \frac{(V_{B,HCL} - V_{A,HCL}) \times C_{HCL}}{m_{lignin}}$$

$$\mathbf{N}[C_6H_5\mathbf{OH}] = \frac{(33,75 - 30,75)[ml] \times 0,1[\frac{mol}{l}]}{0,1[g]}$$

$$\mathbf{N}[C_6H_5\mathbf{OH}] = 3[\frac{mmol}{g}]$$

## Appendix F. Optimization of ABTS concentration

The calculation of a suitable $ABTS^+$ concentration is performed by preparing several diluted test solutions. The $ABTS^+$ was initially diluted with 1:10 and 1:1000 factors, and the absorbance was measured in the UV-Vis spectrophotometer. The goal was to get a maximum peak between 0.700 and 1.00. After measurements, the 1:1000 diluted $ABTS^+$ solution had an absorbance of 0.3 and was therefore too diluted. On the other hand, the 1:10 diluted $ABTS^+$ solution had an absorbance of ~1.1. Therefore, the 1:10 diluted solution was used to calculate the desired concentration using the Beer-Lambert law.

$$\boldsymbol{C_{A\leq 1.000}} = \frac{\boldsymbol{A_{A\leq 1.000}} \times \boldsymbol{C_{1:10\ diluted\ ABTS}}}{\boldsymbol{A_{1:10\ diluted\ ABTS}}} \tag{16}$$

Where, $C_{1:10\ \text{diluted ABTS}}$ is the concentration of ABTS in the $ABTS^+$ solution, and $A_{1:10\ \text{diluted ABTS}}$ is the measured absorbance of the $ABTS^+$ solution. The $C_{A\leq 1.000}$ is the concentration of the $ABTS^+$ in which the solution has an absorbance in the 0.7-1.0 interval at 734 nm. The $A_{A\leq 1.000}$, which is the absorbance equal to 0.7-1.0 interval at 734 nm, was set to 0.8000 in this formula to find out the ABTS concentration, which leads to an absorbance within the mentioned interwall.

After calculating the desired concentration, the 1:10 $ABTS^+$ solution was diluted to the desired concentration.

## Appendix G. Dissolving the Amine SKL lignin at 50 °C

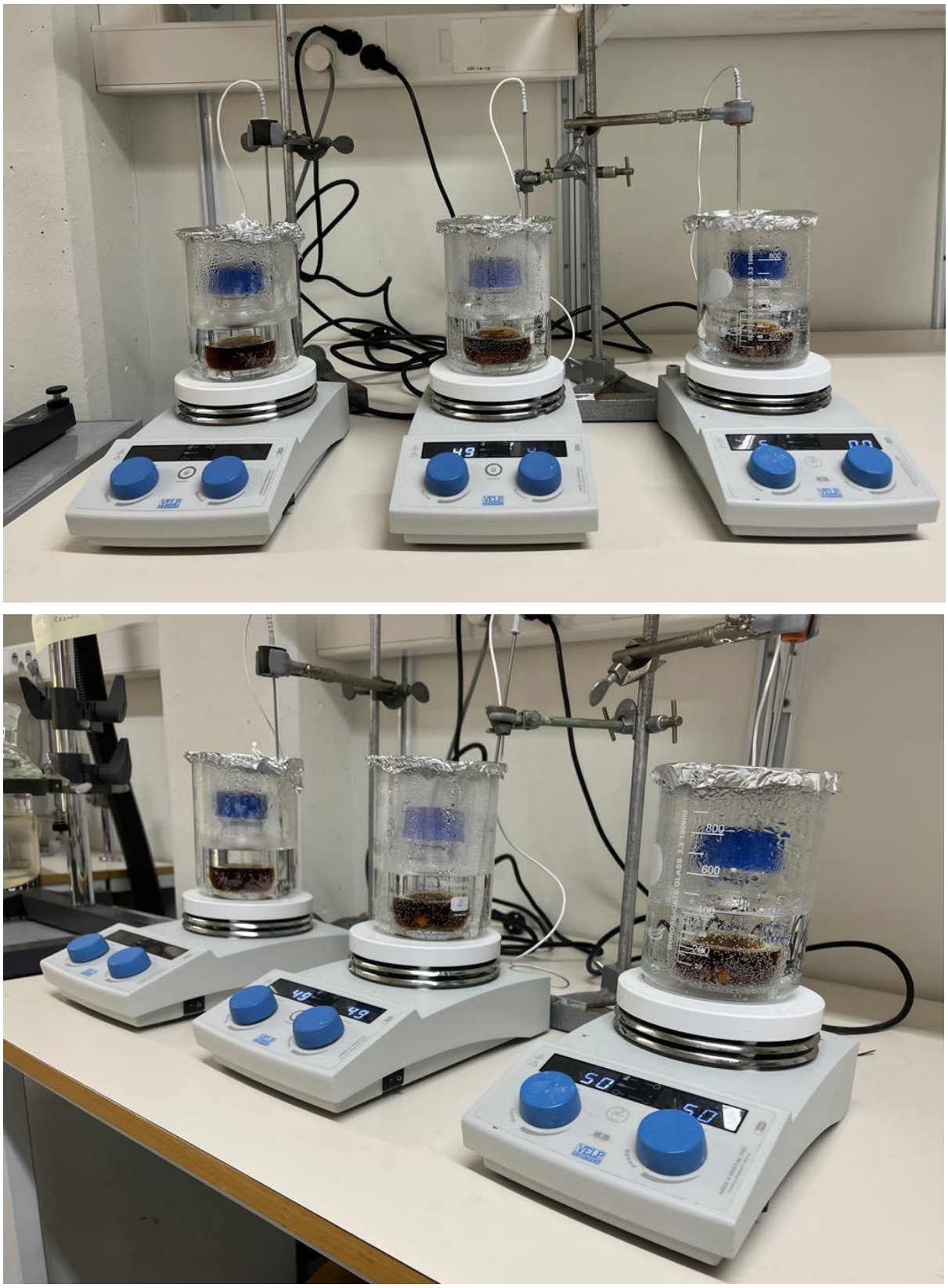

***Figure 23.*** *Set up for dissolving the Amine SKL3 lignin in sodium hydroxide solution (0.1M) by applying heat (~50 °C)*

**DEPARTMENT OF CHEMISTRY AND CHEMICAL ENGINEERING**
**CHALMERS UNIVERSITY OF TECHNOLOGY**
Gothenburg, Sweden 2025
www.chalmers.se


CHALMERS
UNIVERSITY OF TECHNOLOGY